Fission barriers of two odd-neutron actinide nuclei taking into account the time-reversal symmetry breaking at the mean-field level

Meng-Hock Koh, L. Bonneau, P. Quentin, T. V. Nhan Hao, and Husin Wagiran

Phys. Rev. C **95**, 014315 — Published 13 January 2017

DOI: 10.1103/PhysRevC.95.014315

Fission barriers of two odd-neutron actinide nuclei taking into account the time-reversal symmetry breaking at the mean-field level

Meng-Hock Koh,[1,2,3] L. Bonneau,[2,3] P. Quentin,[4,5,2,3,*] T. V. Nhan Hao,[6,7,8] and Husin Wagiran[1]

[1] *Department of Physics, Faculty of Science, Universiti Teknologi Malaysia, 81310 Johor Bahru, Johor, Malaysia*
[2] *University of Bordeaux, CENBG, UMR5797, F-33170 Gradignan, France*
[3] *CNRS, IN2P3, CENBG, UMR5797, F-33170 Gradignan, France*
[4] *Division of Nuclear Physics, Ton Duc Thang University, Ho Chi Minh City, Vietnam*
[5] *Faculty of Applied Sciences, Ton Duc Thang University, Ho Chi Minh City, Vietnam*
[6] *Center of Research and Development, Duy Tan University, K7/25 Quang Trung, Danang, Vietnam*
[7] *Department of Physics and Astronomy, Texas A&M University-Commerce, Commerce, TX 75429, USA*
[8] *Center for Theoretical and Computational Physics, College of Education, Hue University, 34 Le Loi Street, Hue City, Vietnam*

(Dated: December 6, 2016)

Background: Fission barriers of actinide nuclei have been mostly and for long been microscopically calculated for even-even fissioning systems. Calculations in the case of odd nuclei have been performed merely within a so-called equal-filling approximation (EFA) as opposed to an approach taking explicitly into account the time reversal breaking properties at the mean field level- and for only one single-particle configuration.

Purpose: We study the dependence of the fission barriers on various relevant configurations (e.g. to evaluate the so-called specialization energy). Besides, we want to assess the relevance as a function of the deformation of the EFA approach which has been already found out at ground state deformation.

Methods: Calculations within the Hartree-Fock plus BCS with self-consistent particle blocking have been performed using the SkM* Skyrme effective interaction in the particle-hole channel and a seniority force in the particle-particle channel. Axial symmetry has been imposed throughout the whole fission path while the intrinsic parity symmetry has been allowed to be broken in the outer fission barrier region.

Results: Potential energy curves have been determined for six different configurations in ^{235}U and four in ^{239}Pu. Inner and outer fission barriers have been calculated along with some spectroscopic properties in the fission isomeric well. These results have been compared with available data. The influence of time-reversal breaking mean fields on the solutions has been investigated.

Conclusions: A sizeable configuration dependence of the fission barrier (width and height) has been demonstrated. A reasonable agreement with available systematic evaluations of fission barrier heights has been found. The EFA approach has been validated at the large elongations occurring at the outer barrier region.

I. INTRODUCTION

A microscopic understanding of the nuclear fission process remains one of the most complex and challenging problem in low-energy nuclear physics.

Although fission-barrier heights are not observable quantities, they play an important role in determining whether the excited compound nucleus de-excites through neutron evaporation or fission. They are also a necessary input for the calculations of fission cross-sections. From a different point of view, they allow to describe quantitatively the nuclear stability with respect to spontaneous fission in competition with other decay modes, particularly α decay.

Over the years, many microscopic calculations of the average fission paths of heavy nuclei have been performed, within mean-field approaches supplemented by the treatment of nuclear correlations without or with the restoration of some symmetries spuriously broken by the mean-field. While most of fission-barrier calculations have been performed for even-mass (with even proton and neutron numbers) nuclei (see e.g. [1–11] for recent related works), there are comparatively very few microscopic studies dedicated to odd-mass nuclei and even fewer to odd-odd nuclei. The main reason is the complication caused by the breaking of time-reversal symmetry at the mean-field level for a nuclear system involving an odd number of neutrons and/or protons, considered as identical fermions.

One of the earlier microscopic study of spectroscopic properties in odd-mass actinides at very large deformation was performed by Libert and collaborators in Ref. [12] for the band-head energy spectra in the fission-isomeric well of ^{239}Pu within the rotor-plus-quasi-particle approach. More recently, fission-barrier calculations were performed within the Hartree-Fock-Bogoliubov approach by Goriely *et al.* [13] for nuclei with a proton number Z between 88 and 96. The resulting fission barriers were then used for the neutron-induced fission cross-section calculations as part of the RIPL-3 project published in

* Email address:philippe.quentin@tdt.edu.vn

Ref. [14]. Around the same time, Robledo *et al.* have performed fission-barrier calculations of the ^{235}U [15] and ^{239}Pu [16] nuclei, within the equal-filling approximation (EFA) presented e.g. in Ref. [17]. In practice, the EFA consists in occupying pairwise the lowest single-particle energy levels—exhibiting the two-fold Kramers degeneracy—and "splitting" the unpaired nucleon into two time-reversal conjugate states with an equal occupation 0.5. In this way, the time-reversal symmetry is not broken and the calculations are performed in a way which is very similar to what is done when describing the ground state of an even-even nucleus.

There are actually two different formalisms in which this EFA is implemented. One as used in Ref. [15, 16] deals with self-consistent calculations of one quasi particle states. It has been shown to provide the same results as the exact blocking results within this frame for the time-even part of the densities [18]. Another EFA approach will be considered here in some cases for the sake of comparison with the corresponding exact calculations which are the subject of our study. It corresponds here to an equal-filling approximation to self-consistent blocked one-particle states.

Although the EFA is likely to be a reasonable approximation, a proper microscopic description of odd-mass nuclei requires a priori the consideration of all the effects brought up by the unpaired nucleon. This nucleon gives rise to non-vanishing time-odd densities entering the mean-field Hamiltonian. The terms involving time-odd densities vanish identically in the ground-state of even-even nuclei. Their presence for odd-mass nuclei increases the computing task. As discussed for e.g. in Refs. [19, 20], the time-odd densities cause a spin polarisation of the even-even core nucleus which results in the removal of the Kramers degeneracy of the single-particle states. The recent work of Ref. [21] shows that the static magnetic properties of deformed odd-mass nuclei can be properly described when taking into account the effect of core polarization induced by the breaking of the time-reversal symmetry at the mean-field level. Therefore, it is our purpose here to study the effect on fission barriers of the time-reversal symmetry breaking. To do so, we calculate fission-barrier profiles of odd-mass nuclei within the self-consistent blocking approach in the HF+BCS framework, taking the time-reversal symmetry breaking at the mean-field level into account.

As well known, some geometrical intrinsic solutions are broken near both inner and outer barriers. The intrinsic parity is violated for elongations somewhat before the outer barrier region and beyond [22]. The axial symmetry is also known from a very long time to be violated in static calculations around the inner barrier, an effect which is increasing with Z in the actinide region from, e.g., Thorium isotopes [23].

Recently it has been suggested that the outer barrier of actinide nuclei should also correspond to triaxial shapes [24]. However the triaxial character of the fission path in both barriers might vanish or be strongly reduced upon defining it as a least action trajectory upon making some ansatz on adiabatic mass parameters as well as on the set of collective variables to be retained. This has been first discussed in Ref. [25] for super-heavy nuclei. There, all quadrupole and octupole (axial and non-axial) degrees of freedom have been considered. The mass parameters had been calculated according to the Inglis-Belyaev formula [26]. Such a result has been recently confirmed in non-relativistic [27] and relativistic [24, 28] mean-field calculations. The calculations of mass parameters have been significantly improved by using the non-perturbative ATDHFB approach first discussed and used in Ref. [29], later revisited in Ref. [30]. Moreover the intensities of pairing fluctuations have been included in the set of collective variables together with the two axial and non-axial quadrupole degrees of freedom. Calculations in ^{240}Pu and ^{264}Fm in Ref. [27] as well as ^{250}Fm and ^{264}Fm in Ref. [28] have drawn similar conclusions about the disappearance or strong quenching of the triaxiality of the fission paths. These results have been shown to imply very strong consequences on the spontaneous fission half-lives.

¿From these considerations, and keeping in mind the somewhat preliminary character of our exploration of fission barriers of odd nuclei, we have deemed as a reasonable first step to stick here to purely axial microscopic static solutions.

This paper is organized as follows. In Sec. II, a brief presentation of the self-consistent blocking HF+BCS formalism and some of its key aspects are given together with some technical details of the calculations. Our results will be presented in Section III and Section IV. Finally, the main results are summarised and some conclusions drawn in the Section V.

II. THEORETICAL FRAMEWORK

The fission-barrier heights have been obtained from deformation-energy curves whereby the quadrupole moment has been chosen as the driving coordinate. The total energy at specific deformation points has been calculated within the Hartree-Fock-plus-BCS (HF+BCS) approach with blocking, and we refer to this as a self-consistent blocking (SCB) calculation. We will first discuss the details of our SCB calculations in Subsection A, while our approximate treatment for the restoration of rotational symmetry using the Bohr-Mottelson (BM) unified model is presented in Subsection B. A detailed discussion about the expressions relating our mean-field solutions to the BM model can be found in Ref. [31], and we shall only retain the relevant expressions herein. Subsection C will be devoted to the treatment of the moment of inertia entering the rotational energy in the BM model, and Subsection D to some technical aspects of the calculations.

A. Self-consistent-blocking calculations

We assume that the nucleus has an axially symmetrical shape such that the projection Ω_k of the total angular momentum onto the axial symmetry z-axis $\hat{j}_z$ of the single-particle state $|k\rangle$

$$\langle k|\hat{j}_z|k\rangle = \Omega_k \tag{1}$$

is a good quantum number. The intrinsic left-right (parity) symmetry was allowed to be broken around and beyond the top of the outer-barrier, where such a symmetry breaking is known to lower the outer-barrier. For our description of odd-mass nuclei, we have merely considered seniority-1 nuclear states in which only one single-particle state is blocked. The lowest nuclear K^π state, in general, corresponds to an unpaired nucleon blocked in the single-particle state which is the nearest to the Fermi level with quantum numbers such that $\Omega_k = K$ and, when parity symmetry is not broken, $\pi_k = \pi$. In practice, the blocking procedure translates to setting the occupation probability v_k^2 of the blocked single-particle state and its pair-conjugate state to 1 and 0, respectively.

Such a blocking procedure in an odd-mass nucleus results in the suppression of the Kramers degeneracy of the single-particle spectrum. As a consequence of time-reversal symmetry breaking at the mean-field level, the pairs of conjugate single-particle states needed for the BCS pairing treatment cannot be pairs of time-reversed states. However, without recourse to the Bogoliubov treatment, we were able to unambiguously identify pair-conjugate states by searching for the maximum overlap in absolute value between two eigenstates of the mean-field Hamiltonian, $|k\rangle$ and $|\widetilde{k}\rangle$, such that $|\langle k|\big(\hat{T}|\widetilde{k}\rangle\big)|$, where $\hat{T}$ denotes the time-reversal symmetry operator, is as close to 1 as possible. These partner states $|k\rangle$ and $|\widetilde{k}\rangle$ are dubbed as *pseudo-pairs* and they serve as Cooper pairs in our BCS framework. The value for this overlap will be exactly 1 when time-reversal symmetry is not broken. This procedure for establishing the BCS pair states when time-reversal symmetry is broken at the mean-field level has been implemented earlier in the work of Ref. [32]. A more detail discussion can also be found in Appendix A of Ref. [31].

The breaking of the time-reversal symmetry induces terms which are related to the non-vanishing time-odd local densities in the Skyrme energy density functionals (see Appendix A). These time-odd local densities are the spin-vector densities $\mathbf{s}_q$, the spin-vector kinetic energy densities $\mathbf{T}_q$, the current densities $\mathbf{j}_q$ where the index q here represents the nucleon charge states. These time-odd local densities contributes in such a way that the expectation value of the energy is a time-even quantity as it should.

B. Bohr-Mottelson total energy

The total energy within our Bohr-Mottelson approach (see the detailed discussion of Ref. [31]), is written as

$$\begin{aligned}&\langle IMK\pi\alpha|\hat{H}_{\rm BM}|IMK\pi\alpha\rangle \\ &= \langle\Psi^\alpha_{K\pi}|\hat{H}_{\rm eff}|\Psi^\alpha_{K\pi}\rangle - \frac{1}{2\,\mathcal{J}}\langle\mathbf{J}^2\rangle_{\rm core} + \frac{\hbar^2}{2\,\mathcal{J}}\Big[I(I+1) \\ &- K(K-1) + \delta_{K,\frac{1}{2}}a(-1)^{I+\frac{1}{2}}(I+\frac{1}{2})\Big]\end{aligned} \tag{2}$$

with $|IMK\pi\alpha\rangle$ being the normalized nuclear state defined by

$$\begin{aligned}|IMK\pi\alpha\rangle =&\sqrt{\frac{2I+1}{16\pi^2}}\Big[D^I_{MK}|\Psi^\alpha_{K\pi}\rangle \\ &+ (-)^{(I+K)}D^I_{M\,-K}\hat{T}|\Psi^\alpha_{K\pi}\rangle\Big]\end{aligned} \tag{3}$$

In the notation above, I and M are the total angular momentum, and its projection on the symmetry axis in the laboratory frame, respectively. The state $|\Psi^\alpha_{K\pi}\rangle$ refers to the intrinsic nuclear state, while D^I_{MK} is a Wigner rotation matrix. The $\langle\mathbf{J}^2\rangle_{\rm core}$ quantity is the expectation value of the total angular momentum operator for a polarized even-even core. In our model, Coriolis coupling has been neglected except for the case of $K = 1/2$ in which its effect has been accounted for by the decoupling parameter term. The moment of inertia $\mathcal{J}$ and the decoupling parameter a have been computed from the microscopic solution of the polarized even-even core (see Ref. [31]).

For the band-head state ($I = K$), the Bohr-Mottelson total energy reduces to

$$E_{K\pi\alpha} = \langle\hat{H}_{\rm eff}\rangle - \frac{1}{2\,\mathcal{J}}\langle\mathbf{J}^2\rangle_{\rm core} + \frac{\hbar^2}{2\,\mathcal{J}}(2K - \delta_{K,\frac{1}{2}}a) \tag{4}$$

For given quantum numbers K and π (when the intrinsic parity symmetry is present) the fission-barrier heights have then been calculated as differences of the Bohr-Mottelson energy in Eq. (4) at the saddle points and the normally-deformed ground-state K^π solution.

C. Calculation of the moment of inertia

Special attention has been paid to the moment of inertia entering the core rotational energy term given by $\mathrm{E_{rot}} = \langle\hat{\mathbf{J}}^2\rangle_{\rm core}/2\mathcal{J}$. The usual way to handle it is to use the Inglis-Belyaev (IB) formula [26]. It is not satisfactory for at least three reasons. It is derived within the adiabatic limit of the Routhian Hartree-Fock-Bogoliubov approach. The Routhian approach is, as well known, only a semi-quantal prescription to describe the rotation of a quantal object. Moreover, it is not clear, as we will see, that the corresponding collective motion is adiabatic. Finally, the IB formula corresponds to a well-defined approximation to the Routhian-Hartree-Fock-Bogoliubov approach.

Concerning the last point, as discussed in Ref. [29], the IB moment of inertia ought to be renormalized to take into account the so-called Thouless-Valatin corrective terms [33] studied in detail in Ref. [29]. They arise from the response of the self-consistent fields with respect to the time-odd density (as e.g. current and spin vector densities) generated by the rotation of the nucleus which is neglected in the IB ansatz. In order to incorporate these corrective terms in our current approach, the moments of inertia yielded by the IB formula $\mathcal{J}_{\rm Bel}$ are scaled by a factor α whose value is taken to be 0.32 following the prescription of Ref. [34]:

$$\mathcal{J}' \;=\; \mathcal{J}_{\rm Bel}\,(1+\alpha)\,. \tag{5}$$

As a result, one should diminish by the same percentage the rotational correction evaluated upon using the IB moment of inertia. Let us remark that the above correction concerns adiabatic regimes of rotation.

Projecting after variation the 0^+ state out of a HF+BCS solution, corresponds, of course, in principle to a better approach to the determination of the ground-state energy. This has been performed in Ref. [35] for the fission-barrier of ^{240}Pu upon using two Skyrme force parametrizations (SLy4 and SLy6 [36, 37]). These works clearly show that using the IB approach leads to an overestimation of the rotational correction by about 10 - 20% in the region of inner-barrier and fission-isomeric state and by more than 80% close to the outer-barrier. A word of caution on the specific values listed above should be made, however, since these calculations yield a first 2^+ energy in the ground-state band which is about twice its experimental value (83 keV instead of 43 keV).

A third theoretical estimate stems from the consideration of a phenomenological approach belonging to the family of Variable Moment of Inertia models. It describes the evolution of rotational energies in a band by consideration of the well known Coriolis Anti-Pairing (CAP) effect [38] in terms of intrinsic vortical currents (see e.g. Ref. [39]). The IB treatment to the moment of inertia corresponds to a global nuclear rotation which is adiabatic, i.e. corresponding to a low angular velocity Ω, or equivalently to a rather small value of the total angular momentum (also referred to as spin). However, one can compute the average value of the total angular momentum $I_{\rm av}$ spuriously included in the mean-field solution as

$$I_{\rm av}(I_{\rm av}+1)\hbar^2 = \langle \hat{\mathbf{J}}^2 \rangle \tag{6}$$

where $\hat{\mathbf{J}}$ is the total angular momentum operator, and find that the value of $I_{\rm av}$ even at ground-state deformation cannot be considered as small (one finds there that $I_{\rm av} \approx 13$). Consequently, the moment of inertia entering the rotational correction term should reflect the fact that the average Ω is large.

Recently, a polynomial expression for the moment of inertia as a function of Ω denoted as $\mathcal{J}(\Omega)$ has been proposed according to this approach to the Coriolis antipairing effect (see Ref. [40] and a preliminary account of it in Ref. [41]). This model shall be referred to as the Intrinsic Vorticity Model (IVM) in the discussion herein. The IVM was found to work well for the rotational bands in the ground-state deformation for some actinide nuclei, for instance a very good agreement for ^{240}Pu for a value of I as high as $I_{\rm av} \approx 30$ (where it predicts a rotational energy differing by only 70 keV from the experimental value).

TABLE I. Rotational energy (in MeV) calculated from Belyaev formula (IB) and the Intrinsic Vorticity Model (IVM) at the ground-state deformation of four even-even nuclei as a function of the total angular momentum I_{av} defined in Eq. (6).

Nucleus	I_{av}	IB	IVM
^{234}U	12.988	2.371	1.232
^{236}U	12.905	2.423	1.255
^{238}Pu	13.146	2.441	1.266
^{240}Pu	13.143	2.408	1.232

Table I lists the spurious rotational energy obtained with the IB formula as compared to the IVM rotational energy for a given value of the total angular momentum $I_{\rm av}$ in the ground-state of even-even nuclei. In all cases, the spurious rotational energy evaluated with the IB moments of inertia is larger by about a factor of 2 with respect to the values obtained in the IVM approach. Therefore, the rotational energy obtained with the IB formula should be reduced by approximately 50%. The same amount of correction is assumed to apply as well to all other deformations.

Incidentally, the 50% reduction in the rotational energy at all deformation happens to translate into lowerings of fission barriers of the same magnitude as those obtained from the angular momentum projection calculations of Ref. [35] in ^{240}Pu.

One may note that in both the exact or approximate projection formalisms described above, one overlooks -as we will do here- the possible effect of coupling of the pairing mode with the collective shape degrees of freedom, as for instance a possible Coulomb centrifugal stretching (see e.g. Ref. [41]). Indeed, if any, this effect should be more important at the angular momentum value $I_{\rm av}$ than at much lower spins.

In view of this, we consider to fix ideas, the following three approaches to the calculation of the moment of inertia, namely

(i) the Inglis-Belyaev's formula (IB),

(ii) the increase of the Inglis-Belyaev moment of inertia by 32% (IB+32%), in order to take into account the Thouless-Valatin corrective terms,

(iii) the renormalization of the Inglis-Belyaev moment of inertia by a factor of 2 (IB+100%), which arises from the 50% reduction in the rotational energy of the intrinsic vorticity model.

D. Total nuclear energies within an approximate projection on good parity states

In the spirit of the unified model description of odd nuclei disentangling the dynamics of an even-even core on one hand and of the unpaired (odd) nucleon on the other, we factorize the total wavefunction (with an obvious notation) as

$$|\Psi_{tot}\rangle = |\Phi_{core}\rangle|\phi_{odd}\rangle\,. \tag{7}$$

Similarly we decompose the total Hamiltonian in two separate core and single particle parts

$$\hat{H} = \hat{H}_{core}\hat{h}_{odd}\,. \tag{8}$$

Upon projecting on good parity states both core and odd particle states we get

$$|\Psi_{tot}\rangle = |\Psi^+\rangle + |\Psi^-\rangle \tag{9}$$

where the good parity components of $|\Psi_{tot}\rangle$ may be developed onto core and odd-particle good parity components as

$$|\Psi^+\rangle = \epsilon\eta|\Phi^+_{core}\rangle|\phi^+_{odd}\rangle + \sqrt{1-\epsilon^2}\sqrt{1-\eta^2}|\Phi^-_{core}\rangle|\phi^-_{odd}\rangle \tag{10}$$

and similarly

$$|\Psi^-\rangle = \epsilon\sqrt{1-\eta^2}|\Phi^+_{core}\rangle|\phi^-_{odd}\rangle + \sqrt{1-\epsilon^2}\eta^2|\Phi^-_{core}\rangle|\phi^+_{odd}\rangle \tag{11}$$

where all kets on the r.h.s. of the two above equations are normalized. As a result of this, and further making the rough assumption that $\hat{H}_{core}$ and $\hat{h}_{odd}$ break only slightly the parity, one gets approximately the energies of the state described by the ket $|\Psi_{tot}\rangle$ after projection as

$$E^+ = \frac{\epsilon^2\eta^2(E^+_{core}+h^+_{odd}) + (1-\epsilon^2)(1-\eta^2)(E^-_{core}+h^-_{odd})}{1-(\epsilon^2+\eta^2)+2\epsilon^2\eta^2} \tag{12}$$

in the positive parity case and similarly for the negative parity case

$$E^- = \frac{\epsilon^2(1-\eta^2)(E^+_{core}+h^-_{odd}) + (1-\epsilon^2)\eta^2(E^-_{core}+h^+_{odd})}{(\epsilon^2+\eta^2)-2\epsilon^2\eta^2} \tag{13}$$

where E^+_{core} and E^-_{core} are the energies of the projected core states and h^+_{odd} and h^-_{odd} are the diagonal matrix elements $\langle\phi^+_{odd}|\hat{h}_{odd}|\phi^+_{odd}\rangle$ and $\langle\phi^-_{odd}|\hat{h}_{odd}|\phi^-_{odd}\rangle$.

Only in special cases, can we easily approximate from what we know about the core projected energies, what are the total projected energy of the odd nucleus.

Let us illustrate the above in two simple cases. The first one is a favourable one where the odd nucleon has an average parity which is roughly equal to one in absolute value (e.g. such that roughly $\eta = 1$). Then, the total projected energies will be given by

$$E^\pi = E^\pi_{core} + e_{odd} \tag{14}$$

where e_{odd} is the single particle (mean field) energy of the last nucleon. Now, we recall that the energy of the core state projected onto a positive parity is lower than (or equal to) what is obtained when projecting it on a negative parity. Moreover, within the core plus particle approach, we may approximate (à la Koopmans) the total projected nuclear energy $E(K,\pi)$ of the odd nucleus corresponding to a (K,π) configuration for the last nucleon as

$$E(K,\pi) = E^+_{core} + e_{odd} = E_{int}(K,\pi) + \Delta E^+_{core} \tag{15}$$

where the intrinsic total energy $E_{int}(K,\pi)$ results from our microscopic calculations for the considered single particle (K,π) configuration and the corrective energy ΔE^+_{core} is the gain in energy obtained when projecting the core intrinsic solution on its positive parity componenet.

On the contrary whenever the average parity of the odd nucleon state is close to zero such that roughly $\eta^2 = \frac{1}{2}$ one would get for instance for the positive parity projected state

$$E^+ = \frac{\epsilon^2 E^+_{core} + (1-\epsilon^2)E^-_{core}}{2} + \frac{\epsilon^2 h^+_{odd} + (1-\epsilon^2)h^-_{odd}}{2}\,, \tag{16}$$

which cannot be simply evaluated without a detailed knowledge of the projected wave functions.

E. Some technical aspects of the calculations

We have employed the SkM* [42] parametrization as the main choice of the Skyrme force for our calculations. This Skyrme parametrization has been fitted to the liquid drop fission-barrier of ^{240}Pu and is usually considered as the standard parametrization for the study of fission-barrier properties, for e.g in Refs. [11, 43] within the HF framework and Refs. [3, 44, 45] in the Hartree-Fock-Bogoliubov calculations. Two other parametrizations will be also considered here in some cases, namely the SIII [46] and the SLy5* [47] parameter sets.

As was done in the study of low-lying band-head spectra in the ground-state deformation [31], to be consistent with the fitting protocol and respect the galilean invariance, we have neglected the terms involving the spin-current tensor density $J^{\mu\nu}_q$ and the spin-kinetic density $\mathbf{T}_q$ by setting the corresponding coupling constants B_{14} and B_{15} (see Appendix A for the definition of these constants) to 0 in the energy-density functional and the Hartree–Fock mean field. To make this presentation self-contained we recall in Appendix A, the expressions of the Skyrme energy-density functional and the Hartree–Fock fields, together with the coupling constants in terms of the Skyrme parameters. In addition, we have also neglected the terms of the form $\mathbf{s}\cdot\Delta\mathbf{s}$ in the energy-density functional, where $\mathbf{s}$ is the spin nucleon density, and the corresponding terms of the Hartree–Fock Hamiltonian. We shall refer to this as the *minimal time-odd* scheme

where only some combinations of the time-odd densities appearing in the Hamiltonian density are taken into account. On the other hand, the *full time-odd* scheme refers to the case where all time-odd densities are considered when solving the Hartree–Fock equations.

The pairing interaction has been approximated with a seniority force which assumes the constancy of so-called pairing matrix elements between all single-particle states belonging to a restricted valence space. In our case, the valence space has been chosen to include all single-particle states up to $\lambda_{\rm q}+X$, where $\lambda_{\rm q}$ is the chemical potential for the charge state q and $X = 6$ MeV. A smoothing factor of Fermi type with a diffuseness $\mu = 0.2$ MeV (see e.g. Ref. [48] for details) has been used to avoid a sudden variation of the single-particle valence space. The pairing matrix element is given by

$$g_{\rm q} = \frac{G_{\rm q}}{N_{\rm q}+11}\,, \tag{17}$$

where $N_{\rm q}$ denotes the nucleon number of charge state q. The pairing strengths $G_{\rm q}$ were obtained by reproducing as best as possible the experimental mass differences $\Delta_q^{(3)}(N_{\rm q})$ of some well-deformed actinide nuclei (for odd $N_{\rm q}$-values, see Ref. [31] for further discussions). The obtained values when using the SkM* parametrization are $G_{\rm n} = G_{\rm p} = 16.0$ MeV.

The calculated single-particle states have been expanded in a cylindrical harmonic oscillator basis. The expansion needs to be truncated at some point, and this has been performed according to the prescription of Ref. [49]

$$\hbar\omega_\perp\Big(n_\perp+1\Big)+\hbar\omega_z\Big(n_z+\frac{1}{2}\Big)\leq\hbar\omega_0\Big(N_0+2\Big)\,, \tag{18}$$

where the frequencies ω_z and $\omega_\perp$ are related to the spherical angular frequency, ω_0, by $\omega_0^3=\omega_\perp^2\omega_z$. The basis size parameter $N_0 = 14$ which corresponds to 15 spherical major shells has been chosen. The two basis size parameters have been optimized for a given Skyrme interaction at each deformation point of the neighbouring even-even nuclei while assuming axial and parity symmetrical nuclear shapes. The optimized values were then used for the calculations of the odd-mass nuclei.

Numerical integrations were performed using the Gauss–Hermite and Gauss–Laguerre approximations with 16 and 50 mesh points, respectively. The Coulomb exchange term has been evaluated in a usual approximation generally referred to as the Slater approximation [50] even though it had been proposed much earlier by C.F. von Weisæcker [51].

III. FISSION-BARRIER CALCULATIONS

A. Fission barriers of odd-mass nuclei without rotational correction

First the HF+BCS calculations of deformation energy curves as functions of the quadrupole moment Q_{20}, with imposed parity symmetry, were performed in the two even-even neighboring isotopes of a given odd-mass nucleus. Subsequently, the calculations for the odd-mass nucleus were then carried out starting from the converged solutions of either one of the two even-even neighboring nuclei. It has been checked that, as it should, the choice of the initial even-even core solution to be used at a particular deformation point does not affect the solution of the odd-mass nucleus when self-consistency is achieved.

For odd-mass nuclei, the choice of the blocked states have been limited to the low-lying band-head states appearing in the ground-state well. This corresponds to blocking the single-particle states with quantum numbers $\Omega^\pi = 1/2^+$, $5/2^+$, $7/2^-$ and $7/2^+$ for ^{239}Pu and ^{235}U, and the additional two single-particle states with $\Omega^\pi = 3/2^+$ and $5/2^-$ for ^{235}U. In all cases, the single-particle state with the desired K^π quantum numbers nearest to the Fermi level is selected as the blocked state at every step of the iteration process. However, this selection criterion does not guarantee a converged solution. There can be, indeed, a problem related to the oscillation of the blocked state from one iteration to the next. In this case, we were forced to perform, instead, two sets of calculations. The blocked configuration with a lower energy solution was selected as the solution for the particular K^π state.

The results of these calculations where intrinsic parity is conserved are displayed on Figs. 1 (for ^{239}Pu) and 2 (for ^{235}U). They lead as well-known, to unduly high fission barriers for two reasons. One is that a correction for the spurious rotational energy content (as above discussed and substantiated below) should be removed throughout the whole deformation energy curve. The second specific to the outer barrier is related to the imposition of the intrinsic parity symmetry. This is why parity-symmetry breaking calculations have been considered. Due to the huge amount of numerical effort that it involves, we have considered only some of the lower band-head states in the ground-state deformation. These are band-head states with $K = 1/2$, $5/2$ and $7/2$ states for ^{239}Pu, and $1/2$, $3/2$ and two $7/2$ states for ^{235}U. These parity symmetry breaking calculations were performed starting from a converged parity-symmetric solution of the respective K^π configuration beyond the fission-isomeric well. From this initial solution corresponding to a given elongation (as measured by Q_{20}), we blocked one single-particle state with $K = \Omega$ and then performed calculations by constraining the nucleus to a slightly asymmetrical shape at a finite Q_{30} value for a few iterations. The constraint on Q_{30} was then released and the calculations were allowed to reach convergence. Once an asymmetric solution was obtained, we used it for calculating the next Q_{20} deformation point with an increment of 20 barns.

The results of such parity breaking calculations are reported also on Figs. 1 and 2. Figure 3 illustrates on a specific example, the transition from a symmetrical equilibrium solution at $Q_{20} = 95$ b to increasingly asymmetrical equilibrium solutions upon increasing Q_{20}.

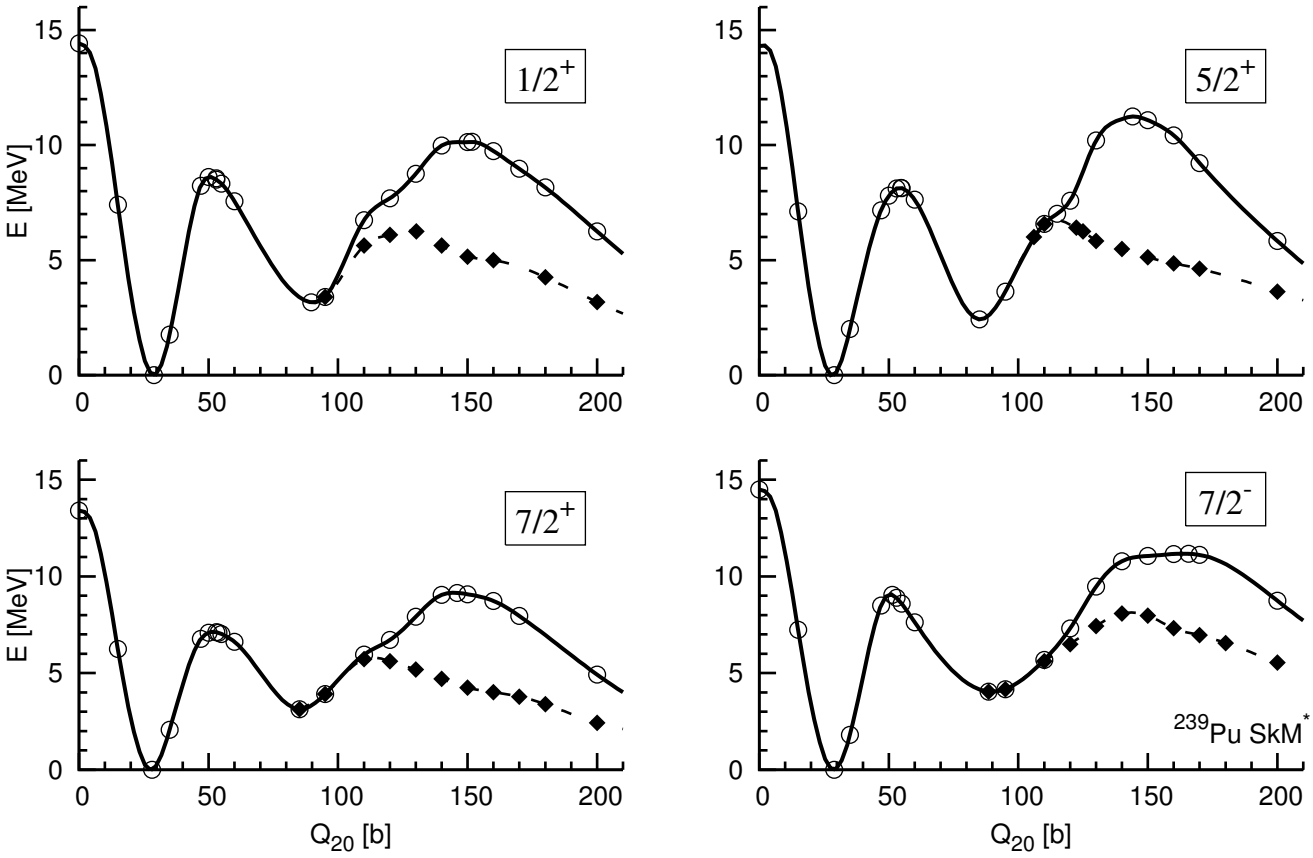

FIG. 1. Deformation energy curves of ^{239}Pu as functions of Q_{20} calculated with the SkM* parametrization and without taking the rotational energy correction into account. The K^π labels refer to the quantum numbers in the parity symmetrical region (unfilled circles). The plotted solutions when this symmetry is broken (filled circles) are obtained by continuity as functions of Q_{20}. .

At the top of the barrier (corresponding roughly to the $Q_{20} = 110 - 130$ b range) the attained octupole deformations (as measured by Q_{30}) reach large values which are representative of the most probable fragmentation in the asymmetrical fission mode experimentally observed at very low excitation energy in this region. Of course, upon releasing the symmetry constraint, the parity is no longer a good quantum number. Thus, e.g. on Fig. 1, the parity-broken energy curve associated with the label $1/2^+$ corresponds merely to a $K = 1/2$ solution beyond the critical point where the left-right reflection symmetry is lost. This may cause some ambiguity in how we define the fission barrier. For instance, in the case of ^{235}U (Fig. 2) we have two $K = 7/2$ solutions of opposite parity. On Fig. 4, we have reported potential energy curves for the two $K = 7/2$ solutions followed by continuity upon increasing the deformation from the parity conserved region. It turns out that the energy curves of these two solutions are crossing around $Q_{20} = 115$ barns. The solution stemming at low Q_{20} from a positive parity configuration becomes energetically favored. We could thus define a lowest $K = 7/2$ fission barrier by jumping from one solution to the other. Yet, this overlooks two problems. One which will be touched upon below, is the projection on good parity states. The other is the fact that we do not allow here for a residual interaction between the two configurations, a refinement that is beyond the scope of our current approach.

As expected, the parity-symmetry-breaking calculations do yield a substantial effect on the intrinsic deformation energies around the outer fission-barrier. Its height for the 1/2 configuration in ^{239}Pu is lowered by about 3.9 MeV with respect to the symmetrical barrier, leading to a calculated height $E_B = 6.3$ MeV. The outer-barrier height for the 5/2 configuration, in the same nucleus, was found to be $E_B = 6.6$ MeV, corresponding to an even larger reduction of 4.7 MeV with respect to the left-right symmetric barrier height. Important reductions of fission barrier heights are also obtained in the ^{235}U case (see Fig. 2). One lowers the $K = 1/2$ outer barrier by 3.7 MeV and by 5.4 MeV in the $K = 7/2$ case.

Associated with this substantial gain in energy upon releasing the left-right reflection symmetry, one observes also a very important lowering of the elongation at the

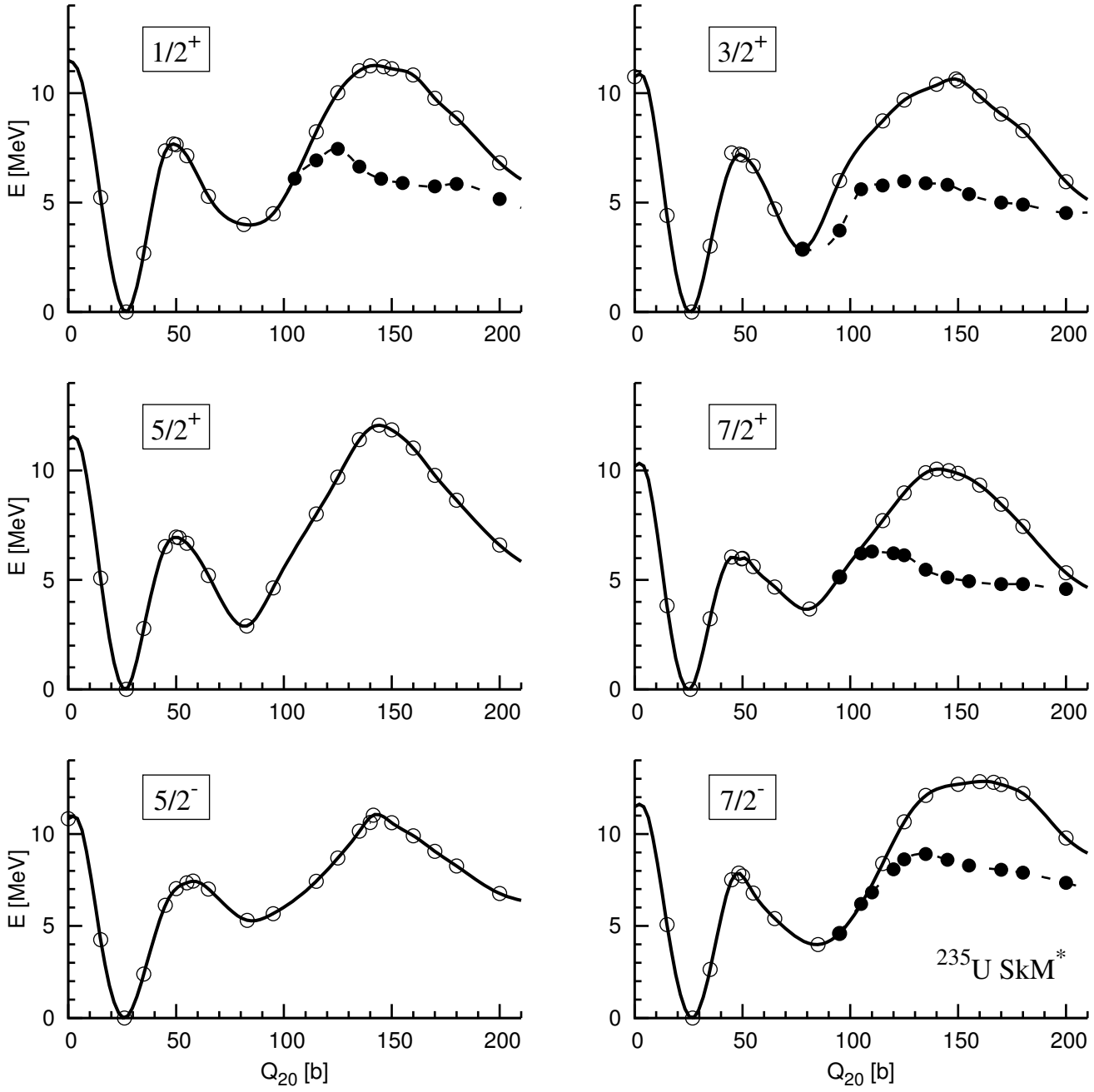

FIG. 2. Same as Fig. 1 for ^{235}U.

outer fission saddle point, resulting in a reduced barrier width and therefore in a strong further enhancement of the barrier penetrability.

To generate relevant outer barrier heights, one has in principle to project our solutions on good parity states. In the absence of such calculations for the odd nuclei under consideration here, one may propose some reasonable estimates taking stock of what we know about the projection of a neighboring even-even core nucleus. As discussed in Subsection II.D however, this is only possi-

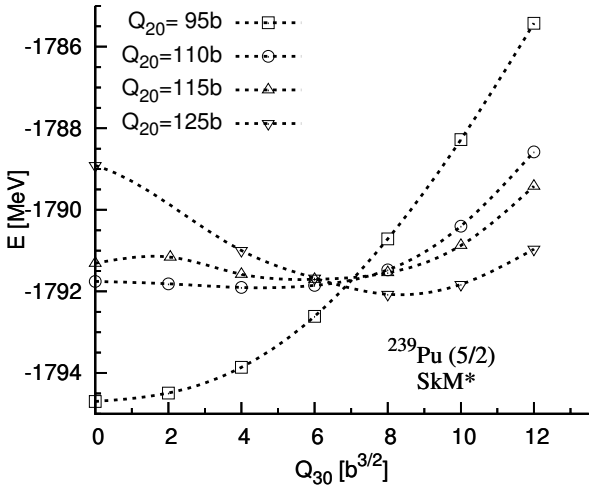

FIG. 3. Cuts for given values of Q_{20} in the potential-energy surface around the top of the outer barrier as a function of the octupole moment Q_{30} (given in barns$^{3/2}$) of the 5/2 blocked configuration of ^{239}Pu. The SkM* parametrization has been used.

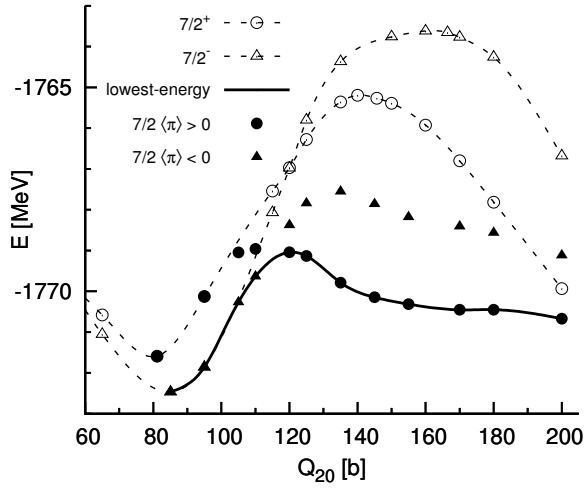

FIG. 4. A portion of the deformation energy curves of the blocked $K = 7/2$ configurations in ^{235}U from the fission-isomeric well up to beyond the top of the outer-barrier. The filled symbols refer to the local minima as a function of Q_{30} for fixed elongation Q_{20} while the unfilled symbols refer to the solutions obtained by imposing a left-right symmetry. The solid line connects the lowest-energy solutions when the left-right symmetry is broken.

ble whenever the single-particle wavefunction of the last (unpaired) nucleon corresponds to an average value of the parity operator which is close to 1 in absolute value. This is not always the case as exemplified on Fig. 5 corresponding to two low excitation energy $K = 7/2$ configurations in the ^{235}U nucleus. They are followed, as we have already seen, by continuity from slightly before the isomeric-fission well to much beyond the outer barrier. One of these two solutions stemming from a $K^\pi = 7/2^-$ configuration at small elongation keeps up to $Q_{20} = 120 - 130$ b an average parity reasonably close to 1. On the contrary, the other $K = 7/2$ solution involves in the outer barrier region, a large mixing of contributions from both parities. We will therefore be only able to evaluate the fission barrier of the former and will not propose any outer fission barrier height for the latter.

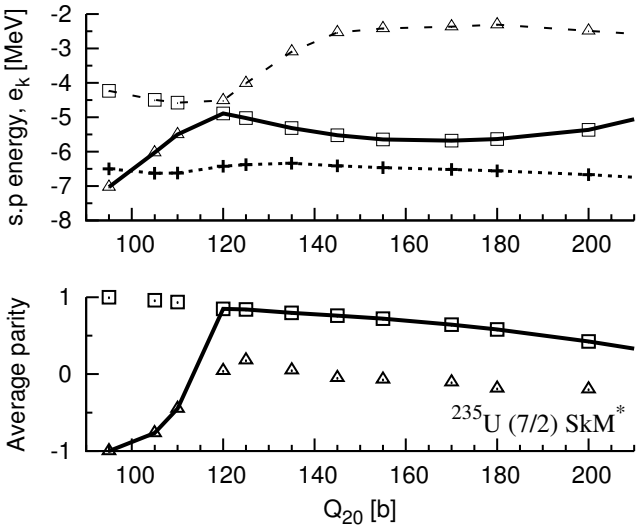

FIG. 5. (Top): Evolution of the single-particle energies for two $\Omega = 7/2$ states near the BCS chemical potential (marked with crosses) as functions of Q_{20} obtained in the parity asymmetric calculations of ^{235}U. The solid line connects the blocked single-particle states as a function of deformation. (Bottom): Average parity of the above considered blocked single-particle states as a function of Q_{20}.

In the work of Ref. [11] one has described the fission barrier of ^{240}Pu nucleus within the Highly Truncated Diagonalization approach, to account for pairing correlations while preserving the particle-number symmetry. Such solutions have been projected on good parity states after variation. The parity-projection calculation had no effect on the total binding energy at the top of the outer fission-barrier, where the value of Q_{30} was found to be very large. In contrast, projecting on a positive parity state causes a lowering of the total binding energy in the fission-isomeric well.

Using the notation of Subsection II.D, one has obtained in Ref. [11] for the ^{240}Pu nucleus, a positive correcting energy Δ^+_{core} about equal to 350 keV for the fission-isomeric state and which vanishes at the top of the outer barrier.

According to the discussion of Subsection II.D, out of all the configurations considered up to the isomeric state in ^{235}U and in ^{239}Pu, only the $K^\pi = 1/2^+$ and $7/2^+$ configurations in ^{235}U, and the $7/2^+$ configuration in ^{239}Pu qualify to allow us to propose reasonable estimates of the

outer fission barrier heights (see Table II).

TABLE II. Expectation value of the parity of the parity operator for the blocked single-particle state nearest to the Fermi level in both considered odd nuclei corresponding to a specific K configuration in the $Q_{20} = 120 - 130$ barn region. The SkM*interaction has been used. Only the lowest energy solutions have been considered for a given K value. In the single case $K = 7/2$ where two solutions stemming by continuity from states with the same K and opposite π values were close enough in energy (a couple of MeV) we have reported the parity expectation value of both, putting in parenthesis the solution with the higher energy.

K	1/2	3/2	5/2	7/2
^{235}U	0.76	−0.53	0.06	0.85 (0.10)
^{239}Pu	–	−0.13	–	0.83 (0.19)

B. Inclusion of rotational energy and sensitivity of fission-barrier heights to the moment of inertia

Table III displays the inner-barrier height E_A, the fission-isomeric energy $E_{\rm IS}$ and the outer-barrier height E_B, obtained within the Bohr-Mottelson unified model (therefore including the rotational energy). Parity symmetric and asymmetric (when available) outer-barrier heights are both tabulated for completeness. It should be emphasized that the notation $E_{\rm IS}$ used here is not synonymous with the usual meaning of fission-isomeric energy often denoted by $E_{\rm II}$. The latter refers to the energy difference between the lowest-energy solutions in the fission-isomeric and ground-state wells. The corresponding results will be reported in Section IV, while the former is the energy difference between given K^π quantum numbers in the two wells.

It can be seen from Table III that the rotational-energy correction calculated using the Inglis-Belyaev formula gives too low an outer fission barrier in some cases, as compared to the empirical values found to be within the range of 5.5 to 6.0 MeV (see Table IV presented in the next Subsection). The increase in the IB moments of inertia by 32% and 100% as discussed in Section II results in an increase, on the average, of E_A and E_{IS} by about 0.27 MeV and 0.35 MeV, respectively while the parity symmetric E_B increases by about 0.64 MeV.

Among the three different considered energy differences, E_B is found to be the most sensitive one to the variation of the moment of inertia as expected in view of the well-known increase of the rotational energy correction with the elongation.

C. Comparison with empirical values and other calculations

Before comparing our fission-barrier heights to other available data, some corrections should be made. The corrections considered herein, stem from approximations of different nature: the so-called Slater approximation to the Coulomb exchange interaction, the truncation of the harmonic-oscillator basis, and the effect of triaxiality around the inner-barrier ignored here.

We shall discuss first the corrections to be made for the inner-barrier heights. A test study on the impact of basis size parameter on the fission-barrier heights is presented in Appendix B. As discussed therein, the inner-barrier height is estimated to be lowered by about 300 keV when increasing the basis size parameter N_0 to a value where this relative energy may be considered to have converged. Moreover the use of Slater approximation was found in Ref. [52] to underestimate the inner-barrier height of ^{238}U by about also 300 keV. Assuming that a similar correction applies to the two considered nuclei irrespective of the K^π quantum numbers, our inner-barrier height should be increased by the same magnitude.

Let us consider the impact of breaking the axial symmetry should around the top of the inner barrier. When breaking this symmetry, K is no longer a good quantum number and this may pose a problem in the blocking procedure for an odd-mass nucleus since the single-particle states will contain to some extent mixtures of K quantum number components. As a simple ansatz, overlooking these potential difficulties, we estimate the lowering of the inner barrier of odd-mass nuclei by using the results obtained in similar triaxial calculations for even-mass nuclei, taking stock of the results of Ref. [56] where the same SkM* parametrization and seniority residual interaction have been used. Thus assuming that the effect of including the triaxiality is the same as in ^{236}U (for ^{235}U) and as in ^{240}Pu (for ^{239}Pu) for all considered blocked configurations, we expect a reduction in the inner-barrier height by about 1.3 MeV.

Taking the three above mentioned corrections into account, we obtain a total reduction of the inner-barrier height by about 1.3 MeV.

Next, we consider the isomeric energies E_{IS}. We estimate that the finite basis size effect (see Appendix B) results in an overestimation of this energy by about 0.5 MeV. The exact Coulomb exchange calculations of Ref. [52] have shown that the Slater approximation yielded an underestimation of the isomeric energy of ^{238}U of about 0.3 MeV.

As for the outer barrier now, exact Coulomb exchange calculations have not been performed—due to corresponding very large computing times—for these very elongated shapes in this region of nuclei. As discussed in Ref. [52] most of the correction comes from an error in estimating the Coulomb exchange contributions in low single-particle level density regimes Therefore as far as E_B is concerned, we assume that this correction depends

TABLE III. Inner-barrier height E_A, fission-isomeric energy $E_{\rm IS}$ (with respect to the ground-state solution), and outer-barrier height E_B for the two considered odd-neutron nuclei. The SkM* parametrization has been used. Three values (in MeV) were given in all cases, corresponding to different prescription for the moments of inertia (see the discussion in Section II).

Nucleus	K^π	E_A			$E_{\rm IS}$			E_B (symmetric)			E_B (asymmetric)		
		IB	IB+32%	IB+100%	IB	IB+32%	IB+100%	IB	IB+32%	IB+100%	IB	IB+32%	IB+100%
^{235}U	$1/2^+$	6.57	6.83	7.11	2.60	2.94	3.30	8.60	9.23	9.90	5.31	5.83	6.38
	$3/2^+$	6.19	6.43	6.69	1.48	1.81	2.16	8.12	8.72	9.37			
	$5/2^+$	5.83	6.09	6.37	1.44	1.78	2.15	9.57	10.17	10.80			
	$5/2^-$	6.32	6.59	6.87	3.97	4.28	4.62	8.21	8.81	9.46			
	$7/2^-$	6.97	7.18	7.41	2.70	3.00	3.32	10.25	10.85	11.49			
	$7/2^+$	4.75	5.04	5.35	2.21	2.55	2.91	7.29	7.93	8.61	4.03	4.54	5.09
^{239}Pu	$1/2^+$	7.43	7.71	7.98	1.70	2.05	2.43	7.63	8.24	8.88			
	$5/2^+$	6.97	7.25	7.54	0.96	1.30	1.67	8.83	9.40	10.00			
	$7/2^-$	8.10	8.32	8.56	2.74	3.05	3.37	8.75	9.32	9.93			
	$7/2^+$	5.90	6.18	6.48	1.72	2.05	2.40	6.63	7.22	7.86	3.80	4.25	4.72

TABLE IV. Comparison between various estimates of the inner E_A and outer-barrier E_B heights (given in MeV) of the two considered odd-neutron nuclei. Our calculated fission-barrier heights corresponding to the experimental K^π quantum numbers, at ground state deformation, are listed in the last column, whereby these values have been obtained after taking the various corrections into account.

Nucleus	K	Ref. [15, 16]		Ref. [53]		Ref. [13]		Ref. [54]		Ref. [55]		present work	
		E_A	E_B	E_A	E_B	E_A	E_B	E_A	E_B	E_A	E_B	E_A	E_B
^{235}U	$1/2^+$	9.0	8.0									5.81	6.18
	$3/2^+$	-	-									5.39	-
	$5/2^+$	-	-	4.20	4.87	5.54	5.80	5.25	6.00	5.9	5.6	5.07	-
	$5/2^-$	-	-									5.57	-
	$7/2^-$	8.5	7.2									6.11	-
	$7/2^+$											4.05	4.89
^{239}Pu	$1/2^+$	11.0	8.5									6.68	-
	$5/2^+$	11.5	9.0	5.73	4.65	5.96	5.86	6.20	5.70	6.2	5.5	6.24	-
	$7/2^-$	11.0	8.5									7.26	-
	$7/2^+$											5.18	4.52

only on the treatment of the ground-state and therefore should be the same as what was obtained for E_A, namely an underestimation of 0.3 MeV. The finite basis size effect, as evaluated in a particular case in Appendix B corresponds to an overestimation of about 0.5 MeV. The nett effect of the corrective terms for the outer-barrier height is therefore a decrease by about 0.2 MeV.

When including all the above corrections and using the doubled moment of inertia (IB+100% scheme), we obtain inner-barrier heights for the different blocked configurations ranging from 5.0 to 6.2 MeV for ^{235}U, and from 5.1 to 7.3 MeV for ^{239}Pu. The left-right asymmetric outer-barrier heights lie within the range of 4.8 to 6.2 MeV for the ^{235}U nucleus, and 4.5 MeV for $7/2^+$ configuration in the ^{239}Pu nucleus.

Some other fission-barrier heights have been also reported for comparison in Table IV. More precisely we consider two sets of calculations, namely the EFA calculations by Robledo and collaborators [15, 16] and the macroscopic-microscopic calculations by Möller [53]. Three sets of evaluated fission-barrier heights are alos listed: those fitted to reproduce the neutron-induced fission cross-sections by Goriely and collaborators [13], those coming from the RIPL-3 [14] database extracted from empirical estimates compiled by Maslov *et al.* [54], and the empirical fission-barrier heights of Bjørnholm and Lynn [55] obtained from the lowest-energy solution at the saddle points irrespective of the nuclear angular-momentum and parity quantum numbers.

Out of these values, only those obtained from Refs. [15, 16] using the Gogny D1S force within the Hartree-Fock-Bogoliubov-EFA framework are directly comparable with our results. In these works, axial symmetry is assumed. The resulting fission-barrier heights are much higher than our calculated values. This is consistent with the rather high fission-barrier heights obtained for the even-even

^{240}Pu nucleus in the earlier work of Ref. [57].

It should be stressed that the rather large differences existing between our results and those reported in Refs. [15, 16] cannot be ascribed to the treatment of the time-reversal symmetry breaking. In fact, we have checked that equal-filling approximation (EFA) calculations (corresponding to a particle and not quasi-particle blocking though) affects the total binding energies by a few hundred keV at most for the parity symmetric case. The resuls of calculations for four different configurations in ^{239}Pu of E_A, E_{IS} and E_B are displayed on Table V. The effect of time-reversal symmetry breaking terms is found to be approximately constant with deformation.

TABLE V. Differences (in keV) betwreen the intrinsic fission-barrier heights ($\Delta E_x = \left(E_x\right)_{EFA} - \left(E_x\right)_{SCB}$ with $x \equiv A, IS, B$) calculated within the EFA and SCB framework for ^{239}Pu with the SkM* parametrization.

K^π	ΔE_A	ΔE_{IS}	ΔE_B
$1/2^+$	-70	-50	-10
$5/2^+$	-10	-20	0
$7/2^+$	-10	-20	-10
$7/2^-$	-10	0	0

The comparison with the other sets of data in Table IV is less straightforward. As was mentioned by Schunck *et al.* in Ref. [45], due to an uncertainty in the empirical fission-barrier heights of about 1 MeV, it is may be illusory to attempt a reprodution of empirical values within less than such an error bar. In our case, the fission-barrier heights calculated with the SkM* parametrization and including the various corrective terms as discussed above, falls easily within this range.

D. Specialization energies

Originally (see Refs. [58, 59]), the concept of specialization energy has been defined as the difference between fission barrier heights of an odd nucleus with respect to those of some of its even-even neighbors. Namely one defines, for instance, the specialization energy for the first (inner) barrier, upon considering ^{239}Pu as a ^{238}Pu core plus one neutron particle, as

$$\Delta E_A^{(p)}(^{239}\mathrm{Pu}, K^\pi) = E_A(^{239}\mathrm{Pu}, K^\pi) - E_A(^{238}\mathrm{Pu}, 0^+)\,, \tag{19}$$

and similarly when considering ^{239}Pu as a ^{240}Pu core plus one neutron hole

$$\Delta E_A^{(h)}(^{239}\mathrm{Pu}, K^\pi) = E_A(^{239}\mathrm{Pu}, K^\pi) - E_A(^{240}\mathrm{Pu}, 0^+)\,. \tag{20}$$

For configurations at the ground state deformation having a very low or zero excitation energy, due to the conservation of quantum numbers preventing to follow the *a priori* lowest energy configurations at s.p. level crossings, one expects that these specialization energies should be positive quantities. This is of course the case for experimentally observed spontaneous fission processes. But this would not hold whenever one would consider configurations which correspond to a high enough excitation energy in the ground state well as we will show in a specific case (see Table VI).

To illustrate this concept Figure 6 and Table VI present the deformation-energy curves and the fission-barrier heights, respectively, with a conserved parity symmetry evaluated within the BM unified model for the four blocked K^π configurations of ^{239}Pu with respect to those of the neighbouring even-even nuclei. We see that the inner and outer-barrier heights for some blocked configurations—the $7/2^-$ configuration being an excellent example—are higher than the one of the two neighboring even-even nuclei as a consequence of fixing K^π quantum numbers along the fission path. In contrast the $7/2^+$ blocked configuration happens to yield lower fission-barrier heights as compared to the two neighboring even-even nuclei. This is so, as above discussed, because the $7/2^+$ configuration is found at a much higher excitation energy in the ground-state deformation well [31] but with a low excitation energy at the saddle points as compared to the other blocked configurations. This results in negative specialization energies, as shown in Table VI.

TABLE VI. Specialization energies defined here as the average of Eq. (19) and (20) for the four blocked configurations of ^{239}Pu (in MeV). The Belyaev's moments of inertia have been increased by a factor of 2.

	K^π			
	$1/2^+$	$5/2^+$	$7/2^+$	$7/2^-$
ΔE_A	0.83	0.39	-0.68	1.41
ΔE_B	0.26	1.38	-0.77	1.31

By way of conclusion, one can state that the fission-barrier profiles (heights and widths) are very much dependent on the K^π quantum numbers.

E. Effect of neglected time-odd terms

In order to probe the effect of the neglected time-odd densities we have performed calculations of the total binding energy as a function of deformation with parity symmetry within the so-called *full time-odd* scheme, from the normal-deformed ground-state well up to the fission-isomeric well. For this study, we have also considered another commonly used Skyrme parameters set, namely the SIII parametrization [46], partly because there, the coupling constants B_{14} and B_{18} driving the terms involving the spin-current tensor density $J_q^{\mu\nu}$ and the Laplacian of the spin density, respectively), are exactly zero. In the *full time-odd* scheme, the B_{14}, B_{15}, B_{18} and B_{19} coupling constants are not set to zero but allowed to take

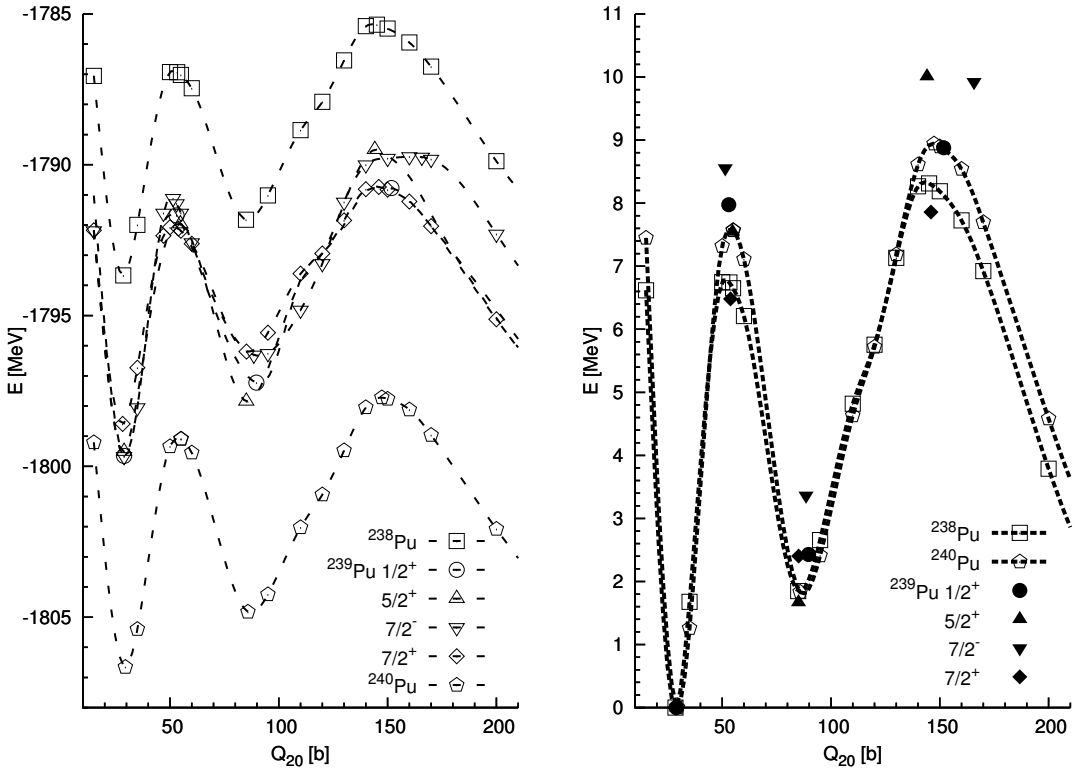

FIG. 6. Deformation-energy curves of ^{238,240}Pu (with $K^\pi = 0^+$) and ^{239}Pu (with $K^\pi = 1/2^+$, $5/2^+$, $7/2^-$ and $7/2^+$) as functions of Q_{20} in barns. The Belyaev's moments of inertia have been increased by a factor of 2. Left panel: absolute energy scale; right panel: relative scale, taking the normal-deformed minimum as the origin of energy for all curves.

the values resulting from their expression in terms of the Skyrme parameters (see Appendix A). The contributions to the inner-barrier height E_A and fission-isomeric energy $E_{\rm IS}$ stemming from the kinetic energy, the Coulomb energy, the pairing energy as well as the various coupling-constant terms appearing in the Skyrme Hamiltonian density are calculated self-consistently in the *minimal* and *full time-odd* schemes from our converged solutions.

More specifically we denote by $\Delta E'_{B_i}$ the difference between the B_i contribution to the inner-barrier heights $\Delta E^{(\rm full)}_{B_i}$ and $\Delta E^{(\rm min)}_{B_i}$ in the *full time-odd* and the *minimal time-odd* schemes, respectively

$$\Delta E'_{B_i} = \Delta E^{(\rm full)}_{B_i} - \Delta E^{(\rm min)}_{B_1} \,. \tag{21}$$

Similarly we denote by $\Delta E^{(\rm full)}_{\rm kin}$ and $\Delta E^{(\rm min)}_{\rm kin}$ the kinetic-energy contribution to the inner-barrier height in both time-odd schemes. In the same spirit the abbreviated indices C and pair are used for the corresponding Coulomb and pairing contributions, respectively. The sum of the double energy differences coming from the kinetic, Coulomb, pairing and B_i contributions with i ranging from 1 to 13 is denoted as $\Delta E'_{\rm min}$

$$\Delta E'_{\rm min} = \Delta E'_{\rm kin} + \sum_{i=1}^{13} \Delta E'_{B_i} + \Delta E'_{\rm pair} + \Delta E'_{\rm C} \,. \tag{22}$$

The difference of inner-barrier heights in the two *time-odd* schemes is therefore given by

$$\Delta E'_A = \Delta E'_{\rm min} + \Delta E'_{B_{14}} + \Delta E'_{B_{15}} + \Delta E'_{B_{18}} + \Delta E'_{B_{19}} \,. \tag{23}$$

Similar notations are used for the fission-isomeric energy.

In Figures 7 and 8, the various energy differences defined above, are represented as histograms for the SkM* and SIII parametrizations, respectively. We find that the inner-barrier heights, in general, decrease when going from a *minimal* to a *full time-odd* scheme in all considered blocked configurations. This is reflected by the negative values of $\Delta E'_A$. The difference in the inner-barrier heights between both time-odd schemes is overall a competition between the $\Delta E'_{\rm min}$ and $\Delta E'_{B_{14,15}}$, while the $\Delta E'_{B_{18,19}}$ terms have a negligible effect. More precisely, the $\Delta E'_{B_{14}}$ term involves the combination of $\overleftrightarrow{J}^2 - \mathbf{s}\cdot\mathbf{T}$ local densities and is found to be dominated by the $\overleftrightarrow{J}^2$ component. When the $\Delta E'_{\rm min}$ and $\Delta E'_{B_{14,15}}$ contributions are of the same magnitude but with opposite signs, then we do not have a change in the inner-barrier height, as is the case for the $7/2^+$ blocked configuration with the SkM* parametrization.

The effect of the time-odd scheme on fission-isomeric energy $E_{\rm IS}$ is less clear-cut. However, we could still ob-

serve that the B_{18} and B_{19} contributions remain negligible. Moreover the time-odd scheme generally has less impact on the fission-isomeric energy than on the inner-barrier height. A notable exception is found for the $1/2^+$ configuration.

This study shows that the terms proportional to coupling constants which are not constrained in the original fits of the Skyrme force can impact the fission-barrier heights in a non-systematic and non-uniform manner. This suggests that one cannot absorb this effect into an adjustment procedure.

IV. SPECTROSCOPIC PROPERTIES IN THE FISSION-ISOMERIC WELL

In this section, we discuss the results obtained in the fission-isomeric well for the ^{235}U and ^{239}Pu nuclei. We will compare here the results obtained with three Skyrme force parametrizations (SkM*, SIII and SLy5*). In the vicinity of the isomeric state, we will make the approximation that the parity mixing is indeed very small, such that (with the notation of Subsection II.D)

$$\epsilon \sim 1 \tag{24}$$

and similarly for an odd nucleon state stemming from a positive parity s.p. configuration

$$\eta \sim 1 \qquad h^+ \sim e_{odd} \qquad h^- \sim 0 \tag{25}$$

while for an odd nucleon state stemming from a negative parity s.p. configuration

$$\eta \sim 0 \qquad h^- \sim e_{odd} \qquad h^+ \sim 0\,. \tag{26}$$

As a result for a positive parity nuclear configuration, the projected energy of the fission-isomeric state will be approximated by

$$E(K^+) \sim E_{int}(K^+) + \Delta E^+_{core} \tag{27}$$

while in the negative parity case we will have

$$E(K^-) \sim E_{int}(K^-) + \Delta E^+_{core} \tag{28}$$

where the intrinsic energies $E_{int}(K^\pm)$ are the energies of our microscopic blocked HF + BCS calculations.

A. Static quadrupole moment

Before discussing relative energy quantities in the fission-isomeric well, we assess the quality of deformation properties of our solutions in this well by calculating the intrinsic quadrupole moments for some relevant K^π configurations in the fission-isomeric well. The obtained values are listed in Table VII. To the best of our knowledge, experimental values are available in ^{239}Pu only [60, 61]. In this nucleus, our values calculated for the $5/2^+$ configuration with the three considered Skyrme force parametrizations are all found to agree with experiment within the quoted error bars.

TABLE VII. Calculated intrinsic quadrupole moments in the isomeric well for the two lowest-energy states in ^{235}U and the two states corresponding to the experimentally known [60, 61] K^π configuration in ^{239}Pu. In addition, the values obtained for the $11/2^+$ state in ^{239}Pu are also reported.

Nucleus	K^π	SkM*	SIII	SLy5*	Exp
^{235}U	$5/2^+$	32.9	31.8	33.4	-
	$11/2^+$	32.5	31.8	32.3	-
^{239}Pu	$5/2^+$	34.1	33.2	34.8	36 ± 4
	$9/2^-$	34.1	33.2	34.5	-
	$11/2^+$	34.5	33.9	34.3	-

B. Fission-isomeric energy, band heads and rotational bands

Above the lowest-energy solution at the fission-isomeric well there are several band-head states within 1 MeV. This has been displayed in Figures 9 and 10 for the ^{239}Pu and ^{235}U nuclei, respectively. These results have been obtained with the inclusion of rotational energy with the approximate Thouless-Valatin corrective term in the moment of inertia (assuming a 32 % increase above the IB value).

Let us first discuss the energy spectra for the ^{239}Pu nucleus for which a comparison with the experimental data of Refs. [62, 63] is possible. As shown in Fig. 9, the experimental ground-state quantum numbers in the normal-deformed well are $1/2^+$ while in the fission-isomeric well they are $5/2^+$. Our calculated results with the SkM* and the SIII parametrizations reproduce these data.

On the contrary, the calculations with the SLy5* parameter set, fail to do it as they yield a $5/2^+$ ground-state in the normal-deformed well located 160 keV below the $1/2^+$ state and a $1/2^+$ lowest-energy state in the fission-isomeric well. Moreover, the $K^\pi = 9/2^-$ state calculated with SLy5* appears at a too high excitation energy of more than 500 keV as compared to the experimental value of about 200 keV.

In contrast the excitation energy of this $9/2^-$ state is found in much better agreement with data for SkM* and SIII (139 keV and 127 keV, respectively). The agreement with the data of these values is expected to be favorably improved when including the effect of Coriolis coupling, as suggested from the work of Ref. [12]. In addition, a $11/2^+$ excited state is predicted at 151 keV, 129 keV and 299 keV with the SLy5*, the SkM* and the SIII parametrizations, respectively. This state was also predicted (at a 44 keV excitation energy) in the Hartree–Fock–Bogoliubov calculations with the Gogny force by Iglesia and collaborators [16].

The rotational band built on the $5/2^+$ band-head state can also be compared with experimental data: the calculated energies for the first two excited states are found to be rather similar within the three considered Skyrme parametrizations in use, and to compare very well with

data.

Let us now move the discussion to the results for the ^{235}U nucleus displayed in Fig. 10. To the best of our knowledge, there are no experimental data available for comparison with our calculated values in the superdeformed well of this nucleus. There are, however, some calculations performed with the Gogny force in the work of Ref. [15] which predict a $5/2^+$ ground state with a first $11/2^+$ excited state at 120 keV in the fission-isomeric well. The same level sequence is also obtained in our calculations with the SkM* and the SLy5* Skyrme parametrizations, although the $11/2^+$ state is located at a much higher energy in the latter parametrization. The calculations with SIII yields the opposite level sequence, with a $5/2^+$ state 66 keV above the $11/2^+$ ground-state.

C. Fission-isomeric energies

Let us discuss now the fission-isomeric energy $E_{\rm II}$. Table VIII displays the fission isomeric energies $E_{\rm II}$ defined as the difference between the energies of the solutions lowest in energy in both the ground state and fission-isomeric wells (irrespective of their K^π quantum numbers), namely with an obvious notation

$$E_{\rm II} = E_0^{\rm IS} - E_0^{\rm GS}\,. \tag{29}$$

As seen on Table VIII (see also Figs. 9 and 10) when using the standard Thouless-Valatin correction of 32% over the IB estimate, the Skyrme SIII interaction yields values of $E_{\rm II}$ which are much too high. This is not very surprising in view of the well-known defect of its surface tension property. On the contrary, the too low value obtained with the SkM* interaction which provides very good Liquid Drop Model barrier heights must be explained by some inadequate account of relevant shell effect energies. The last interaction (SLy5*) provides reasonable $E_{\rm II}$ values (yet slightly too weak).

Now, as discussed before, rotational energy corrections calculated using the Belyaev moment of inertia were found to be too large, resulting in an underestimation of the fission-barrier heights. This is partly due to the resulting overestimation of the rotational correction. As a rough cure for this, one may increase the IB moments of inertia by a factor of 2. The resulting $E_{\rm II}$ values are listed in Table VIII. It has been checked that the band-head energy spectra in the fission-isomeric well are then only affected by some tens of keV from the values shown in Figs. 9 and 10. The K^π quantum numbers of the lowest-energy solutions in all cases remain unchanged except for ^{235}U with the SkM* interaction. In this case, we have a change in the level ordering of the ground and first excited states, where the quoted value of $E_{\rm II} = 2.20$ MeV involves the $K^\pi = 11/2^+$ blocked configuration in the fission-isomeric well.

V. CONCLUDING REMARKS

¿From the above calculations of fission barriers in odd-mass nuclei within a self-consistent blocking approach we can draw the following conclusions.

First, barrier heights and fission isomeric energies depend on the time-odd scheme in a non-systematic way. Indeed they are found to vary with the nucleus and with the quantum numbers in a given nucleus between zero and almost 0.8 MeV in the studied nuclei. This effect cannot be absorbed in the adjustment of the Skyrme parameters. In particular the calculated specialization energies strongly vary with the K and π quantum numbers and can be negative when the blocked configuration lies rather high in energy in the ground-state well and rather low at the saddle point.

Moreover, the equal-filling approximation, defined in our work as an equal occupation of the block single-particle state and its time-reversed state as opposed to the definition of Ref. [18] based on one-quasi-particle states, is found to have no significant effect on deformation and is a fairly good approximation to calculate relative energies, such as the fission-barrier heights and fission-isomeric energies.

Regarding spectroscopic properties in the ground-state and fission-isomeric wells, we have found overall a fair agreement with available data. This gives us some confidence in the deformation properties of the fissioning nuclei, especially in the barrier profiles as functions of the K^π quantum numbers.

In this context, we recall that we have imposed axial symmetry throughout the whole potential energy curve so that the K quantum number remains meaningful. As already discussed, this may be deemed as a reasonable assumption in view of dynamical calculations performed for ^{240}Pu and heavier nuclei, showing that the least-action path is closer to an axial path than the triaxial static one around the top of the inner and outer barriers [25, 27, 28]. Moreover, as far as class I states are concerned, it has been established from gamma decay of even-even and odd-odd rare earth nuclei formed by neutron capture, that the K-quantum number is reasonably conserved even at energies resulting from neutron capture in the thermal and resonance energy domains (see, e.g., [64]).

Regardless of the validity of the axial symmetry assumption, our calculations of fission barriers with fixed K values allow to expect that the penetrabilities of inner and outer fission barriers will strongly vary with the blocked configurations, resulting in a widespread distribution of fission-transmission coefficients as a function of K and π for a fixed J quantum number. This can a priori impact the fission cross section computed in the optical model for fission with the full K mixing approximation (see, for instance, [65, 66]).

As a matter of fact fission cross section calculations require in principle the knowledge of penetrabilities for each discrete transition state, that is the barrier profile

TABLE VIII. Fission-isomeric energy $E_{\rm II}$ for three different prescriptions for the moment of inertia. The K^π quantum numbers of the ground-state solution in the fission-isomeric well are those displayed in Figs. 9 and 10, except for ^{235}U with the SkM* parametrization and when increasing the Belyaev's result by a factor of 2 (column labeled IB+100%), for which the $K^\pi = 11/2^+$ blocked configuration has been considered.

Nucleus	SLy5*			SkM*			SIII			Exp
	IB	IB+32%	IB+100%	IB	IB+32%	IB+100%	IB	IB+32%	IB+100%	
^{235}U	2.36	2.73	3.11	1.46	1.83	2.20	3.62	3.97	4.35	-
^{239}Pu	2.30	2.69	3.10	1.08	1.43	1.80	3.42	3.84	4.30	3.1

and inertia parameters for each discrete state at barrier tops. In Fig. 11 we show such transition states as rotational bands built on various low-lying blocked configurations. They are calculated in the above discussed Bohr–Mottelson approach using Skyrme-HFBCS intrinsic solutions with self-consistent blocking. This kind of results can provide microscopic input to the discrete contribution to the fission transmission coefficients, along the lines of Ref. [13]. Note that, in this work, odd-mass nuclei were not considered in a time-reversal symmetry breaking approach and that the inertia parameters were calculated within a hydrodynamical model. A natural extension, requiring very long computing times, is to compute these parameters from a microscopic model as in the non-perturbative ATDHFB approach [29], consistently with the barrier profiles for each blocked configuration.

Finally, it is to be noted that in such dynamical calculations, and even in static calculations, the phenomenological quality of the pairing interaction is of paramount importance. In our case, its intensities have been determined by a fit based on explicit calculations of odd-even mass differences in the actinide region. However, such approaches suffer a priori from the deficiencies inherent to a non-conserving particle-number theoretical framework, particularly so if strong pairing fluctuations are to be considered. To cure for that in an explicit and manageable fashion, we intend to perform similar calculations as those presented here, using the so called Highly Truncated Diagonalization Approach of Ref. [48].

Appendix A: Skyrme energy density functional

As well known, when using an effective internucleon interaction of the Skyrme type, the total energy of a normalized Slater determinant $|\Psi_{HF}\rangle$ can be written as an integral of a Hamiltonian density, $\mathcal{H}$, such that:

$$E = \langle\Psi_{HF}|\hat{H}|\Psi_{HF}\rangle = \int \mathcal{H}(\mathbf{r})\, d\mathbf{r} = \int \Big(\mathcal{H}_{kin}(\mathbf{r}) + \mathcal{H}_c(\mathbf{r}) + \mathcal{H}_{DD}(\mathbf{r}) + \mathcal{H}_{s.o}(\mathbf{r}) + \mathcal{H}_{Coul}(\mathbf{r})\Big) d\mathbf{r} \tag{A1}$$

where the various Hamiltonian densities $\mathcal{H}_{kin}$, $\mathcal{H}_c$, $\mathcal{H}_{DD}$, $\mathcal{H}_{s.o}$ and $\mathcal{H}_{Coul}(\mathbf{r})$ are given [67, 68] by (see Table IX for the definition of the coefficients B_i as function of the usual t_i, x_i and W_0 parameters of the Skyrme interaction in use)

$$\mathcal{H}_{kin}(\mathbf{r}) = \Big(1 - \frac{1}{A}\Big)\frac{\hbar^2}{2m}\tau \tag{A2}$$

$$\begin{aligned}\mathcal{H}_c(\mathbf{r}) = {} & B_1\rho^2 + B_{10}\mathbf{s}^2 + B_3(\rho\tau - \mathbf{j}^2) + B_{14}(\overleftrightarrow{J}^2 - \mathbf{s}\cdot\mathbf{T}) + B_5\rho\triangle\rho + B_{18}\mathbf{s}\cdot\triangle\mathbf{s} \\ & + \sum_q \{B_2\rho_q^2 + B_{11}\mathbf{s}_q^2 + B_4(\rho_q\tau_q - \mathbf{j}_q^2) + B_{15}\big(\overleftrightarrow{J}_q^{\,2} - \mathbf{s}_q\cdot\mathbf{T}_q\big)\} + B_6\rho_q\triangle\rho_q + B_{19}\mathbf{s}_q\cdot\triangle\mathbf{s}_q\end{aligned} \tag{A3}$$

$$\mathcal{H}_{DD}(\mathbf{r}) = \rho^\alpha\Big[B_7\rho^2 + B_{12}\mathbf{s}^2 + \sum_q (B_8\rho_q^2 + B_{13}\mathbf{s}_q^2)\Big] \tag{A4}$$

$$\mathcal{H}_{s.o}(\mathbf{r}) = B_9\Big[\rho\nabla\cdot\mathbf{J} + \mathbf{j}\cdot\nabla\times\mathbf{s} + \sum_q \big(\rho_q\nabla\cdot\mathbf{J}_q + \mathbf{j}_q\cdot\nabla\times\mathbf{s}_q\big)\Big] \tag{A5}$$

$$\mathcal{H}_{Coul}(\mathbf{r}) \approx \frac{1}{2}\rho_p(\mathbf{r})V_{CD}(\mathbf{r}) - \frac{3}{4}e^2\Big(\frac{3}{\pi}\Big)^{\frac{1}{3}}\rho_p^{\frac{4}{3}}(\mathbf{r}) \tag{A6}$$

The factor $(1 - \frac{1}{A})$ appearing in the kinetic energy density is a corrective term introduced to approximately eliminate the center-of-mass motion spuriously introduced by the breaking of the translational invariance inherent to the mean-field approach. Such an approach has been noted to overestimate the contribution from the center-of-mass correction [69]. Nevertheless, the approximate treatment of the correction term is consistent with the manner in which the adopted Skyrme parametrizations were fitted. For a study on the various approximations of the center-of-mass correction in the mean-field approach and also its effects on nuclear properties as deformation energy surface we refer to Ref. [70].

The direct part of the Coulomb mean field V_{CD} is readily calculated from the proton density (see for the numerical method in use, e.g. Refs. [71–73]). The exchange part given by the second term of equation (A6) has been approximated here as usually done, with a Slater approximation [50]. The effect of using such an approximation as opposed to performing rather time-consuming exact Coulomb exchange calculations have been previously investigated (see Ref. [52, 74, 75]). It has been found that the appropriateness of the Slater approximation is directly related with the proton single-particle level density near the Fermi level, being less good for a spherical (close shell) nucleus as compared to a well deformed nucleus. Consequently, the lowering of the total energy is lesser at the top of the barrier due to a higher single-particle level density when the Slater approximation is more appropriate as compared to the ground-state solution. This translates into an underestimation of the fission-barrier heights when calculations of the Coulomb exchange term are performed using the Slater approximation.

All the above Hamiltonian densities are time-even functionals of the local densities that are further categorized into time-even and time-odd densities with respect to the action of the time-reversal operator. The time-even densities are the particle density $\rho(\mathbf{r})$, the kinetic energy density $\tau(\mathbf{r})$ and the spin-current density $J_{\mu\nu}(\mathbf{r})$ whose explicit definition can be found in Refs. [67, 68].

For each of the time-even densities, there exists a time-odd counterpart, namely the spin density $\mathbf{s}(\mathbf{r})$, the spin kinetic density, $\mathbf{T}_\mu(\mathbf{r})$ and the current density $\mathbf{j}(\mathbf{r})$ (see Refs. [67, 68]).

The Hartree-Fock equations obtained by varying the total energy given in equation (A1) with respect to the single-particle wavefunctions ϕ_k yield the following one-body Hamiltonian $\hat{h}_{HF}$ [67, 68]

$$\begin{aligned}\langle \mathbf{r}|\hat{h}^{(q)}_{HF}|\phi_k\rangle = & -\nabla\cdot\Big(\frac{\hbar^2}{2m^*_q(\mathbf{r})}\nabla[\phi_k](\mathbf{r})\Big) + \Big(U_q(\mathbf{r}) + \delta_{qp}U_{Coul}(\mathbf{r})\Big)[\phi_k](\mathbf{r}) + i\mathbf{W}_q(\mathbf{r})\cdot\Big(\sigma\times\nabla[\phi_k](\mathbf{r})\Big) \\ & - i\sum_{\mu,\nu}\Big\{\Big(W^{(J)}_{q,\mu\nu}(\mathbf{r})\sigma_\nu\nabla_\mu[\phi_k](\mathbf{r})\Big) + \nabla_\mu\Big(W^{(J)}_{q,\mu\nu}(\mathbf{r})\sigma_\nu[\phi_k](\mathbf{r})\Big)\Big\} - \frac{i}{2}\Big\{\mathbf{A}_q(\mathbf{r})\cdot\nabla[\phi_k](\mathbf{r}) \\ & + \nabla\cdot\Big(\mathbf{A}_q[\phi_k](\mathbf{r})\Big)\Big\} + \mathbf{S}_q(\mathbf{r})\cdot\sigma[\phi_k](\mathbf{r}) - \nabla\cdot\Big(\big(\mathbf{C}_q(\mathbf{r})\cdot\sigma\big)\nabla[\phi_k](\mathbf{r})\Big) \end{aligned} \tag{A7}$$

The fields m^*, U_q, U_{Coul}, $\mathbf{W}_q$ and $W^{(J)}_{q,\mu\nu}$ where the notation q labels the nuclear charge state, are time even-operators wheras the fields $\mathbf{S}_q$, $\mathbf{A}_q$ and $\mathbf{C}_q$ are time-odd operators. They are given as follows [67, 68] in terms of the various densities by

TABLE IX. Definition of the coupling constants B_i entering the expression of Hamiltonian densities, in terms of usual Skyrme force parameters.

$B_1 = \frac{t_0}{2}(1+\frac{x_0}{2})$	$B_2 = -\frac{t_0}{2}(\frac{1}{2}+x_0)$	$B_3 = \frac{1}{4}[t_1(1+\frac{x_1}{2}) + t_2(1+\frac{x_2}{2})]$
$B_4 = -\frac{1}{4}[t_1(\frac{1}{2}+x_1) - t_2(\frac{1}{2}+x_2)]$	$B_5 = -\frac{1}{16}[3t_1(1+\frac{x_1}{2}) - t_2(1+\frac{x_2}{2})]$	$B_6 = \frac{1}{16}[3t_1(\frac{1}{2}+x_1) + t_2(\frac{1}{2}+x_2)]$
$B_7 = \frac{t_3}{12}(1+\frac{x_3}{2})$	$B_8 = -\frac{t_3}{12}(\frac{1}{2}+x_3)$	$B_9 = -\frac{W_0}{2}$
$B_{10} = \frac{1}{4}t_0x_0$	$B_{11} = -\frac{1}{4}t_0$	$B_{12} = \frac{1}{24}t_3x_3$
$B_{13} = -\frac{t_3}{24}$	$B_{14} = -\frac{1}{8}(t_1x_1 + t_2x_2)$	$B_{15} = \frac{1}{8}(t_1 - t_2)$
$B_{18} = -\frac{1}{32}(3t_1x_1 - t_2x_2)$	$B_{19} = \frac{1}{32}(3t_1 + t_2)$	

$$\frac{\hbar^2}{2m_q^*} = \frac{\hbar^2}{2m_q} + B_3\rho + B_4\rho_q \tag{A8}$$

$$\begin{aligned} U_q = {} & 2\big(B_1\rho + B_2\rho_n\big) + B_3\tau + B_4\tau_q + 2\big(B_5\Delta\rho + B_6\Delta\rho_q\big) + (2+\alpha)B_7\rho^{1+\alpha} \\ & + B_8\big(\alpha\rho^{(\alpha-1)}\big(\rho_n^2+\rho_p^2\big) + 2\rho^\alpha\rho_q\big) + B_9\big(\nabla\cdot\mathbf{J} + \nabla\cdot\mathbf{J_q}\big) + \alpha\rho^{\alpha-1}\big(B_{12}\mathbf{s}^2 + B_{13}\big(\mathbf{s}_n + \mathbf{s}_p^2\big)\big) \end{aligned} \tag{A9}$$

$$U_{Coul} = V_{dir} - e^2\,\big(\frac{3}{\pi}\rho_p\big)^{1/3} \tag{A10}$$

$$\mathbf{W}_q = -B_9\big(\nabla\rho + \nabla\rho_q\big) \tag{A11}$$

$$W_{q,\mu\nu} = B_{14}J_{\mu\nu} + B_{15}J_{q,\mu\nu} \tag{A12}$$

$$\mathbf{S}_q = 2\big(B_{10} + B_{12}\rho^\alpha\big)\mathbf{s} + 2\big(B_{11} + B_{13}\rho^\alpha\big)\mathbf{s}_q - B_9\nabla\times\big(\mathbf{j}+\mathbf{j}_q\big) - B_{14}\mathbf{T} - B_{15}\mathbf{T}_q + 2\big(B_{18}\Delta s + B_{19}\Delta s_q\big) \tag{A13}$$

$$\mathbf{A}_q = -2\big(B_3\,\mathbf{j} + B_4\,\mathbf{j}_q\big) + B_9\nabla\times\big(\mathbf{s}+\mathbf{s}_q\big) \tag{A14}$$

$$\mathbf{C}_q = -\Big(B_{14}\,\mathbf{s} + B_{15}\,\mathbf{s}_q\Big) \tag{A15}$$

Appendix B: Effect of basis size on fission-barrier heights

The single-particle states of the canonical basis are expanded on deformed harmonic oscillator basis states truncated according to the deformation-dependent truncation scheme of Ref. [49]. ¿From the oscillator frequencies $\omega_\perp$,ω_z one defines a spherical frequency ω_0 by $\omega_0^3 = \omega_z\omega_\perp^2$. The corresponding basis parameters $b = \sqrt{\frac{m\omega_0}{\hbar}}$ and $q = \frac{\omega_\perp}{\omega_z}$ are optimized to yield the minimal energy given a basis size, N_0. For computational time reasons, the calculations are performed with a basis size defined by $N_0 = 14$ corresponding to 15 major shells in the spherical case. The b and q parameters for the calculations involving the SIII and SkM* interactions in odd-mass nuclei are deduced as an average of the optimized basis of its neighbouring even-even isotopes, at each deformation points. It was furthermore checked that the optimal parameter values obtained for the SkM* interaction were applicable for the SLy5* parameters sets up to a very good approximation (of the order of tens of

TABLE X. Inner-barrier E_A, fission-isomeric energy (E_{II} for even-even nucleus and E_{IS} for odd-mass nucleus) and outer-barrier E_B heights of ^{239}Pu and ^{240}Pu assuming axial and intrinsic parity symmetries for different harmonic oscillator basis sizes calculated with the SkM* interaction. All energies are given in MeV.

Nucleus	N_0	E_A	E_{IS} /E_{II}	E_B
^{239}Pu ($5/2^+$)	14	8.14	2.42	11.25
	16	7.97	2.22	10.83
	18	7.93	2.12	10.80
^{240}Pu	14	8.18	2.53	10.18
	16	8.00	2.31	9.76
	18	7.96	2.22	9.71

keV).

In this Appendix we assess the basis size effect on fission-barrier heights using the notation of Subsection II.E. In practice we have performed such a study for the ^{239}Pu and ^{240}Pu nuclei, assuming axial and parity symmetry along the whole fission path. Calculations were performed with the SkM* interaction for three basis sizes (N_0 = 14, 16, 18). It would be a priori desirable to optimize the b and q parameters for each basis size. However, the work of Ref. [43] comparing solutions which has been optimized in their respective basis size, has shown that the impact of the optimization process on the barrier heights is rather small in determining the considered basis size effect. Thus, the same b and q parameters obtained in the optimization process in $N_0 = 14$ have been used for other N_0 values. The locations of the saddle points as well as the ground states and second minima in the deformation energy surface were obtained by using the modified Broyden's method [76].

The fission-barrier heights obtained for the various basis sizes are shown in Table X. The truncation effect are shown to increase with deformation. As a result we have crudely estimated for all considered nuclei (even-even or odd) that the calculations performed with a basis defined by $N_0 = 14$ overestimate on the average, the inner-barrier height by about 300 keV and the isomeric energy as well as the outer-barrier height by about 500 keV.

ACKNOWLEDGMENTS

M.H.K would like to thank Universiti Teknologi Malaysia for the financial support throughout his doctoral study. This research is funded by the Foundation for Science and Technology Development of Ton Duc Thang University (FOSTECT), website: http://fostect.tdt.edu.vn, under Grant FOSTECT.2015.BR.014. Another T.V.N.H. acknowledges the support by the U.S. NSF Grant No. 1415656 and U.S. DOE Grant No. DE-FG02-08ER41533. P.Q. gratefully acknowledges the support of Dr. Wan Saridan for his stay in UTM during the preparation of this paper using his research grant GUP No. 4F501 and of the SCAC of the French Embassy in Kuala Lumpur.

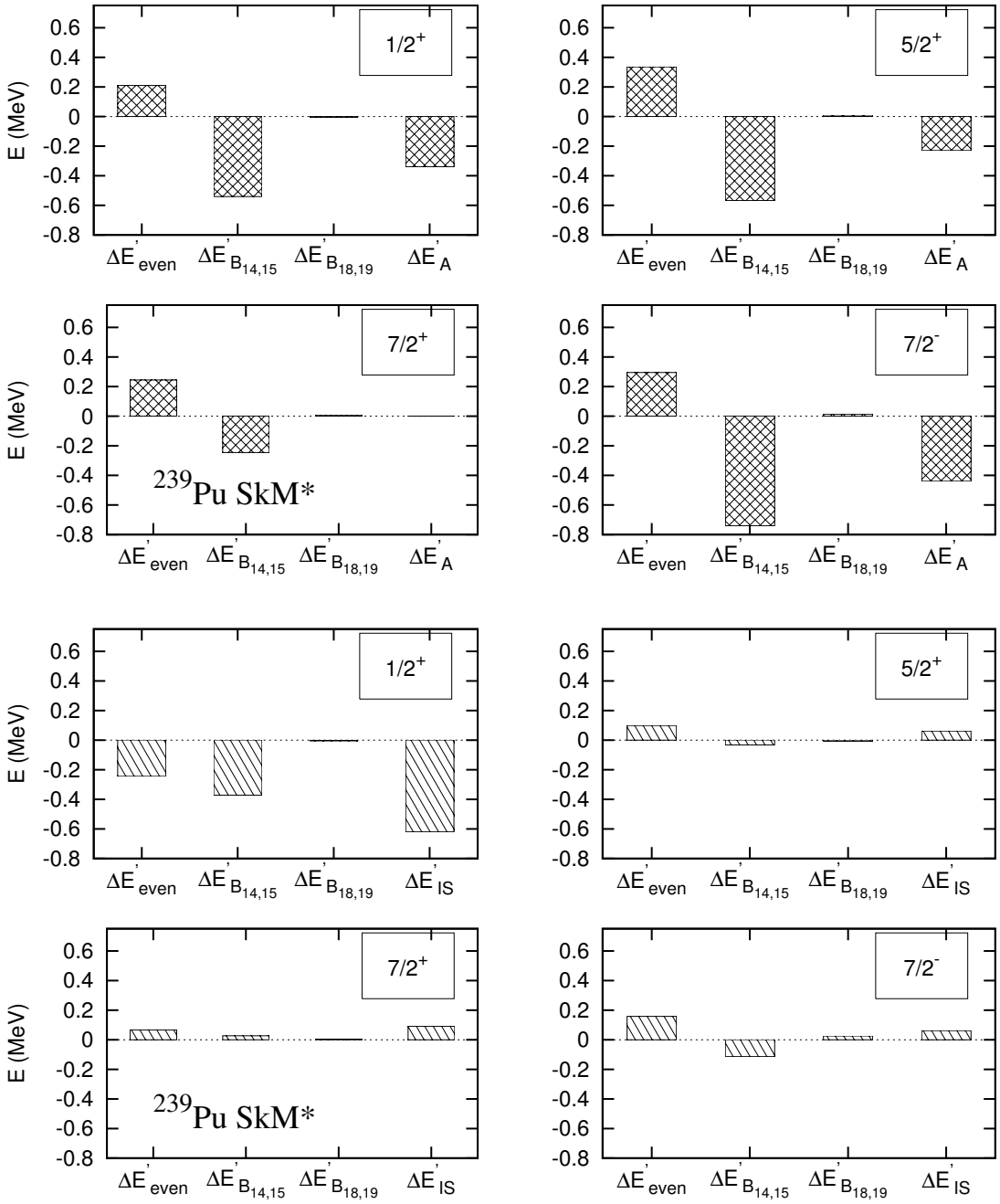

FIG. 7. Energy differences between various contributions (see Eqs. (21) to (23) for definitions) to the inner-barrier height and isomeric energy obtained in the default *minimal time-odd* scheme and the *full time-odd* scheme for several blocked configurations in ^{239}Pu with the SkM* parametrization. The difference in the inner-barrier heights $\Delta E_A^{'}$ and fission-isomeric energy $\Delta E_{\rm IS}^{'}$ between the two schemes are also given for each blocked configuration.

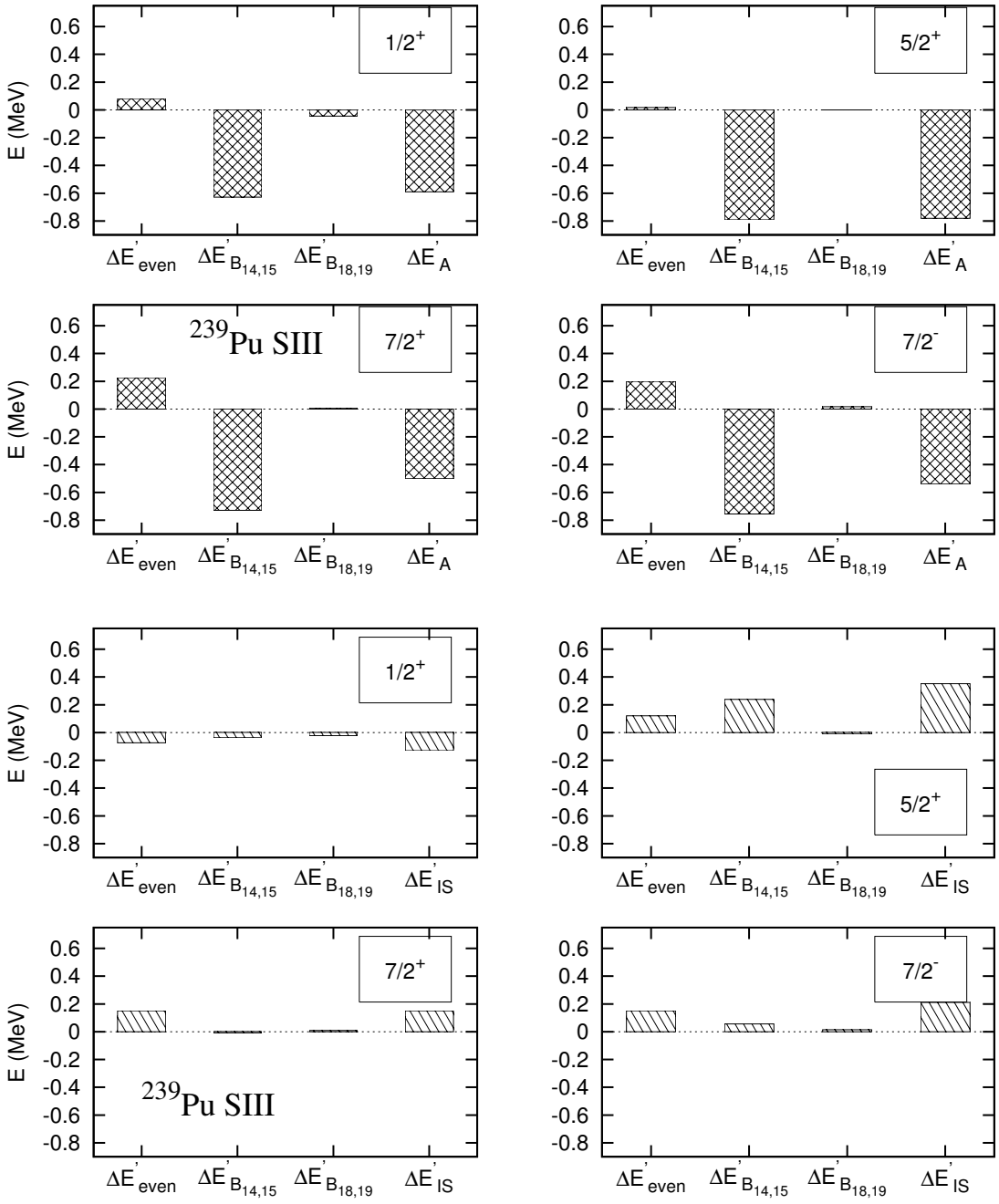

FIG. 8. Same as Figure 7 for the SIII parametrization.

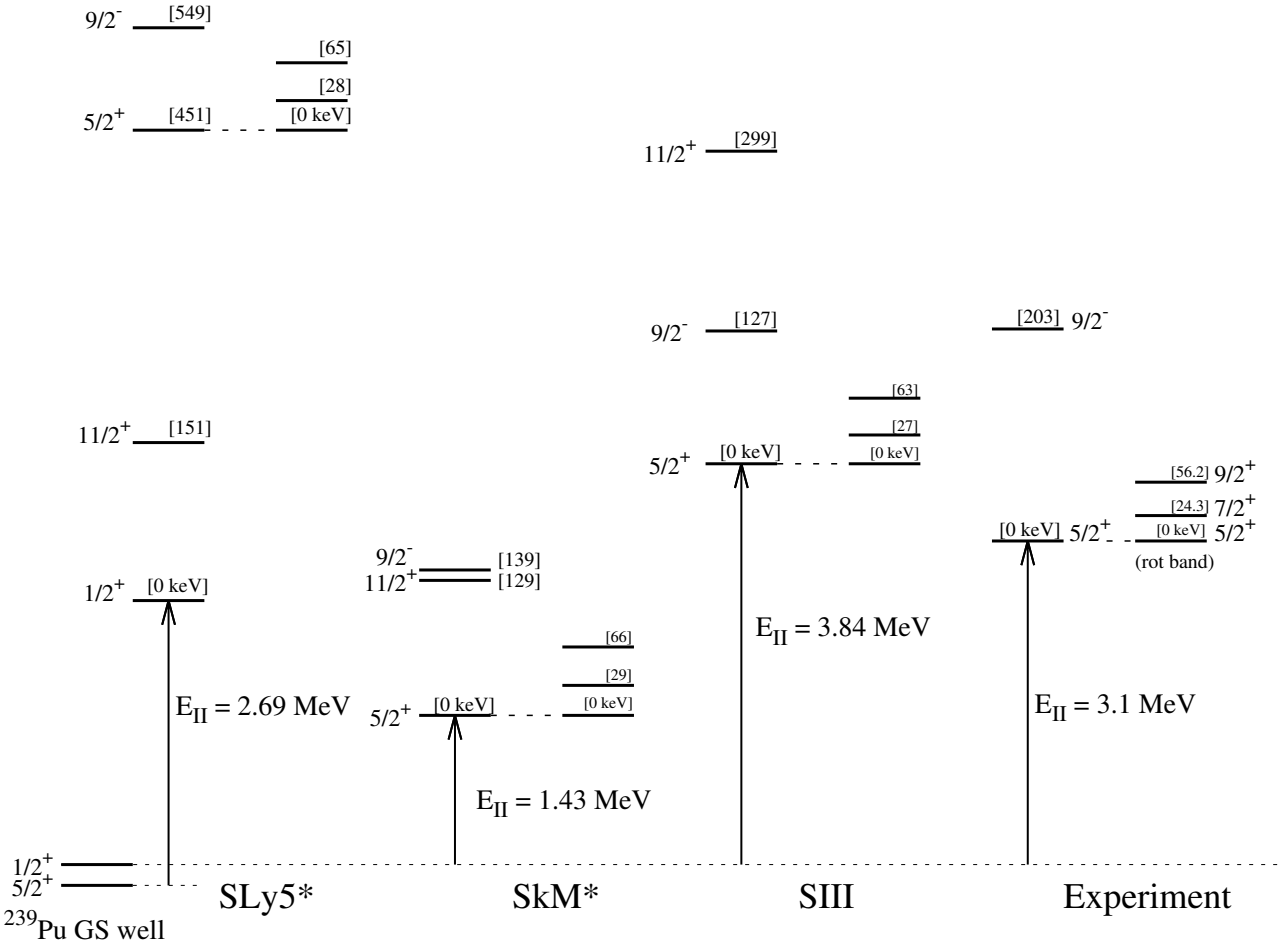

FIG. 9. Band-head energy spectra of ^{239}Pu calculated with the SLy5*, SkM* and SIII parametrizations in the isomeric well with the inclusion of the rotational correction. The standard Thouless-Valatin correction of Ref. [34] beyond the Belyaev's result has been taken into account for the moments of inertia of each band. The rotational spectra built upon the lowest-energy $5/2^+$ state *(rot band)* are also shown on the second column of each Skyrme force. The experimental data are taken from Refs. [62, 63]. The fission-isomeric energy defined as the energy difference between the lowest-energy solution in the ground state and the fission-isomeric well is denoted by $E_{\rm II}$.

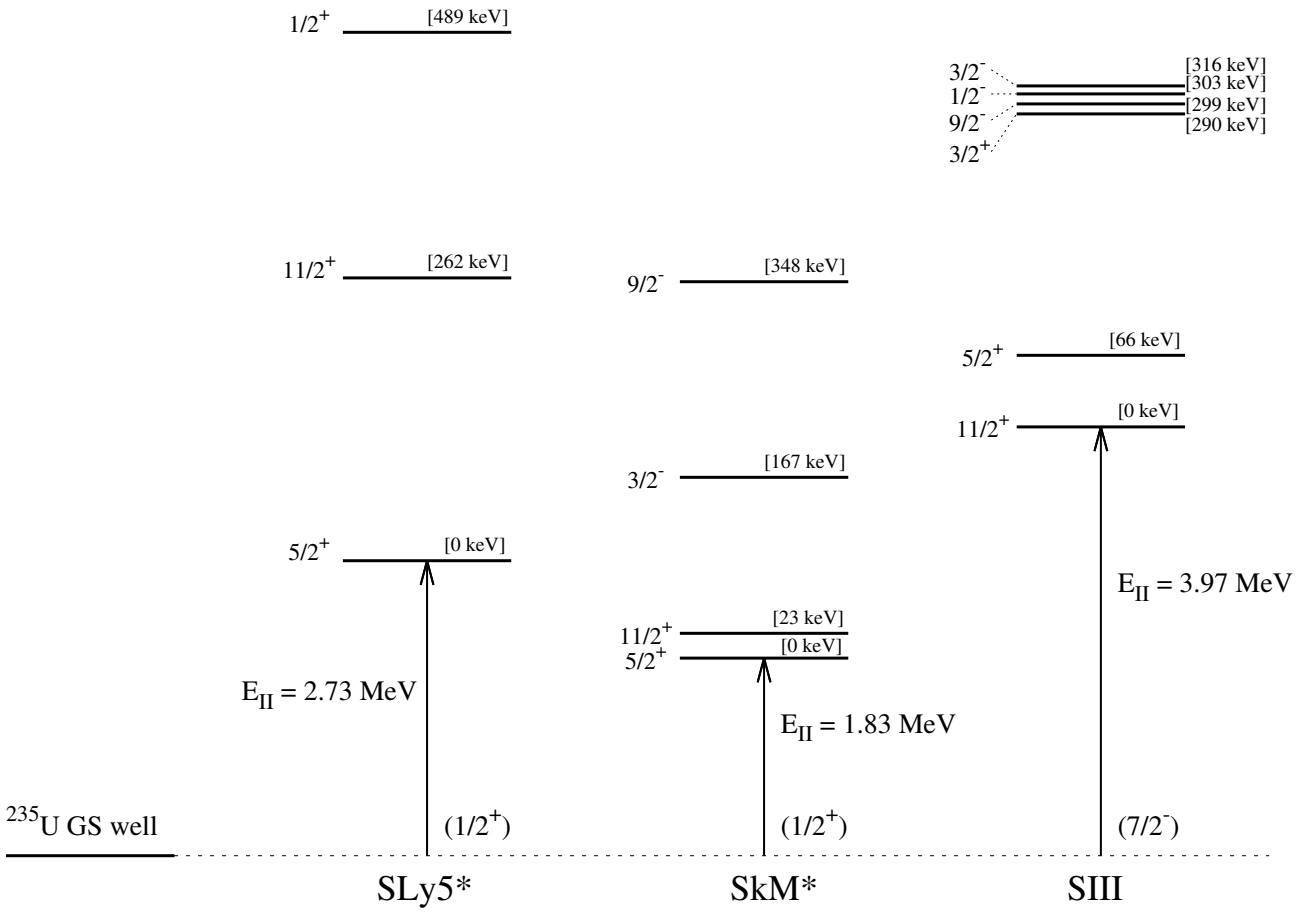

FIG. 10. Same as Figure 9 for ^{235}U.

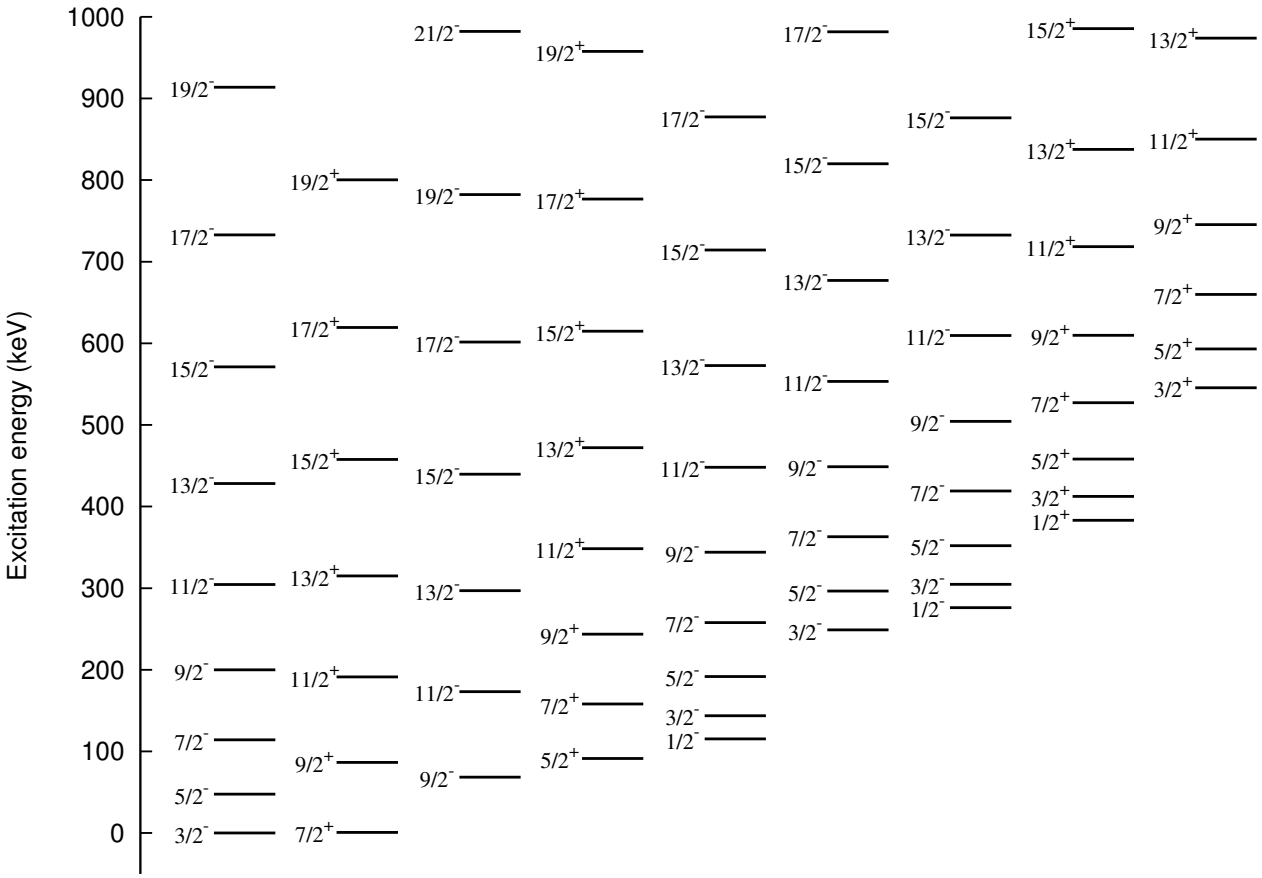

FIG. 11. Example of calculated transition states at the top of the inner barrier of ^{239}Pu.

[1] N. Nikolov, N. Schunck, W. Nazarewicz, M. Bender, and J. Pei, Phys. Rev. C **83**, 034305 (2011).
[2] J. D. McDonnell, W. Nazarewicz, and J. A. Sheikh, Phys. Rev. C **87**, 054327 (2013).
[3] A. Staszczak, A. Baran, and W. Nazarewicz, Phys. Rev. C **87**, 024320 (2013).
[4] W. Younes and D. Gogny, Phys. Rev. C **80**, 054313 (2009).
[5] M. Warda and J. L. Egido, Phys. Rev. C **86**, 014322 (2012).
[6] R. Rodriguez-Guzman and L. M. Robledo, Phys. Rev. C **89**, 054310 (2014).
[7] H. Abusara, A. V. Afanasjev, and P. Ring, Phys. Rev. C **82**, 044303 (2010).
[8] B.-N. Lu, E.-G. Zhao, and S.-G. Zhou, Phys. Rev. C **85**, 011301 (2012).
[9] H. Abusara, A. V. Afanasjev, and P. Ring, Phys. Rev. C **85**, 024314 (2012).
[10] A. V. Afanasjev and O. Abdurazakov, Phys. Rev. C **88**, 014320 (2013).
[11] T. V. N. Hao, P. Quentin, and L. Bonneau, Phys. Rev. C **86**, 064307 (2012).
[12] J. Libert, M. Meyer, and P. Quentin, Phys. Lett. B **95**, 175 (1980).
[13] S. Goriely, S. Hilaire, A. J. Koning, M. Sin, and R. Capote, Phys. Rev. C **79**, 024612 (2009).
[14] R. Capote, M. Herman, P. O. zinsk y, P. G. Young, S. Goriely, T. Belgya, A. V. Ignatyuk, A. J. Koning, S. Hilaire, V. A. Plujko, M. Avrigeanu, O. Bersillon, M. Chadwick, Z. G. T. Fukahori, Y. Han, S. Kailas, J. Kopecky, V. Maslov, G. Reffo, M. Sin, E. S. Soukhovitskii, and P. Talou, Nucl. Data Sheets. **110**, 3107 (2009).
[15] S. Perez-Martin and L. Robledo, Int. J. Mod. Phys. E. **18**, 788 (2009).
[16] F. de la Iglesia, V. Martin, S. Perez-Martin, and L. Robledo, in *Fourth International Workshop on Nuclear Fission and Fission-Product Spectroscopy, Cadarache, France, 13-16 October 2009*, Vol. 1175, edited by A. Chatillon, H. Faust, G. Fioni, D. Goutte, and H. Goutte (AIP Conf. Proc., Melville, NY, 2010) p. 199.
[17] S. Perez-Martin and L. M. Robledo, Phys. Rev. C. **78**, 014304 (2008).
[18] N. Schunck, J. Dobaczewski, J. McDonnell, J. More, W. Nazarewicz, J. Sarich, , and M. V. Stoitsov, Phys. Rev. C **81**, 024316 (2010).
[19] P. Quentin, L. Bonneau, N. Minkov, and D. Samsœn, Int. J. Mod. Phys. E **19**, 611 (2010).
[20] L. Bonneau, J. L. Bloas, P. Quentin, and N. Minkov, Int. J. Mod. Phys. E **20**, 252 (2011).
[21] L. Bonneau, N. Minkov, D. D. Duc, P. Quentin, and J. Bartel, Phys. Rev. C **91**, 054307 (2015).
[22] P. Möller and S. G. Nilsson, Phys. Lett. B **31**, 283 (1970).
[23] V. V. Pashkevich, Nucl. Phys. A **133**, 400 (1969).
[24] B.-N. Lu, J. Zhao, E.-G. Zhao, and S.-G. Zhou, Phys. Rev. C **89**, 014323 (2014).
[25] R. A. Gherghescu, J. Skalski, Z. Patyk, and A. Sobiczewski, Nucl. Phys. A **651**, 237 (1999).
[26] S. T. Belyaev, Nucl. Phys. A **24**, 322 (1961).
[27] J. Sadhukhan, J. Dobaczewski, W. Nazarewicz, J. A. Sheikh, and A. Baran, Phys. Rev. C **90**, 061304(R) (2014).
[28] J. Zhao, B.-N. Lu, T. Nikšić, D. Vretenar, and S.-G. Zhou, Phys. Rev. C **93**, 044315 (2016).
[29] E. K. Yuldashbaeva, J. Libert, P. Quentin, and M. Girod, Phys. Lett. B **461**, 1 (1999).
[30] A. Baran, J. A. Sheikh, J. Dobaczewski, W. Nazarewicz, and A. Staszczak, Phys. Rev. C **84**, 054321 (2011).
[31] M.-H. Koh, D. D. Duc, T. V. N. Hao, T. L. Ha, P. Quentin, and L.Bonneau, Eur. Phys. J. A **52**, 3 (2016).
[32] K. J. Pototzky, J. Erler, P.-G. Reinhard, and V. O. Nesterenko, Eur. Phys. J. A **46**, 299 (2010).
[33] D. J. Thouless and J. G. Valatin, Nucl. Phys. A **31**, 211 (1962).
[34] J. Libert, M. Girod, and J. P. Delaroche, Phys. Rev. C **60**, 054301 (1999).
[35] M.Bender, P.-H.Heenen, and P.Bonche, Phys. Rev. C **70**, 054304 (2004).
[36] E. Chabanat, P. Bonche, P. Haensel, J. Meyer, and R. Schaeffer, Nucl. Phys. A **643**, 441 (1998).
[37] E. Chabanat, P. Bonche, P. Haensel, J. Meyer, and R. Schaeffer, Nucl. Phys. A **635**, 231 (1998).
[38] B. R. Mottelson and J. G. Valatin, Phys. Rev. Lett. **5**, 511 (1960).
[39] P.Quentin, H.Lafchiev, D.Samsœn, and I.N.Mikhailov, Phys. Rev. C **69**, 054315 (2004).
[40] P. Quentin and J. Bartel, to be submitted.
[41] B. Nerlo-Pomorska, K. Pomorski, P. Quentin, and J. Bartel, Phys. Scr. **89**, 054004 (2014).
[42] J. Bartel, P. Quentin, M. Brack, C. Guet, and H.-B. Haakansson, Nucl. Phys. A **386**, 79 (1982).
[43] L. Bonneau, P. Quentin, and D. Samsœn, Eur. Phys. J. A **21**, 391 (2004).
[44] A. Baran, M. Kowal, P.-G. Reinhard, L. Robledo, A. Staszczak, and M. Warda, Nucl. Phys. A **944**, 442 (2015).
[45] N. Schunck, D. Duke, H. Carr, and A. Knoll, Phys. Rev. C **90**, 054305 (2014).
[46] M. Beiner, H. Flocard, N. V. Giai, and P. Quentin, Nucl. Phys. A **238**, 29 (1975).
[47] A. Pastore, D. Davesne, K. Bennaceur, J. Meyer, and V. Hellemans, Phys. Scr. T **154**, 014014 (2013).
[48] N. Pillet, P. Quentin, and J. Libert, Nucl. Phys. A **697**, 141 (2002).
[49] H. Flocard, P. Quentin, A. K. Kerman, and D. Vautherin, Nucl. Phys. A **203**, 433 (1973).
[50] J. C. Slater, Phys. Rev. **81**, 385 (1951).
[51] C. von Weizsæcker, Zeit. Phys. **96**, 431 (1935).
[52] J. L. Bloas, M.-H. Koh, P. Quentin, L. Bonneau, and J. I. A. Ithnin, Phys. Rev. C **84**, 014310 (2011).
[53] P. Möller, A. J. Sierk, T. Ichikawa, A. Iwamoto, R. Bengtsson, H. Uhrenholt, and S. Aberg, Phys. Rev. C **79**, 064304 (2009).
[54] G. N. Smirenkin, *Preparation of Evaluated Data for a Fission Barrier Parameter Library for Isotopes with Z = 82 - 98, with Consideration of the Level Density Models Used*, Tech. Rep. IAEA Report No. INDC(CCP)-359 (IAEA, 1993).
[55] S. Bjørnholm and J. E. Lynn, Rev. Mod. Phys. **52**, 725 (1980).
[56] K. Benrabia, M. Imadalou, D. E. Medjadi, and P. Quentin, to be published.
[57] J. F. Berger, M. Girod, and D.Gogny, Nucl. Phys. A

428, 23c (1984).
[58] J. A. Wheeler, *Niels Bohr and the Development of Physics*, edited by W. Pauli (Pergamon, Oxford, 1955).
[59] J. O. Newton, Prog. Nucl. Phys. **4**, 234 (1955).
[60] D. Habs, V. Metag, H. J. Specht, and G. Ulfert, Phys. Rev. Lett. **38**, 387 (1977).
[61] H. Backe, L. Richter, D. Habs, V. Metag, J. Pedersen, P. Singer, and H. J. Specht, Phys. Rev. Lett. **42**, 490 (1979).
[62] E. Browne and J. Tuli, Nucl. Data Sheets **122**, 293 (2014).
[63] E. Browne, Nucl. Data Sheets **98**, 665 (2003).
[64] L. Bergholt, M. Guttormsen, J. Rekstad, and T. S. Tveter, Phys. Rev. C **50**, 493 (1994).
[65] M. Sin, R. Capote, and A. Ventura, Phys. Rev. C. **74**, 014608 (2006).
[66] M. Sin and R. Capote, Phys. Rev. C. **77**, 054601 (2008).
[67] Y. M. Engel, D. M. Brink, K. Goeke, S. J. Krieger, and D. Vautherin, Nucl. Phys. A **249**, 215 (1975).
[68] P. Bonche, H. Flocard, and P. H.Heenen, Nucl. Phys. A **467**, 115 (1987).
[69] M. Bender, P.-H. Heenen, and P.-G. Reinhard, Rev. Mod. Phys. **75**, 143 (2003).
[70] M. Bender, K. Rutz, P.-G. Reinhard, and J.A.Maruhn, Eur. Phys. J. A **7**, 467 (2000).
[71] D. Vautherin, Phys. Rev. C **7**, 296 (1973).
[72] D. Samsœn, P. Quentin, and J. Bartel, Nucl. Phys. A **652**, 34 (1999).
[73] L. Bonneau, *Fission des noyaux lourds : étude microscopique des barrières de fission et du moment angulaire des fragments.*, Ph.D. thesis, Université Sciences et Technologies - Bordeaux I, (2003).
[74] C. Titin-Schnaider and P. Quentin, Phys. Lett. B **49**, 397 (1974).
[75] J. Skalski, Phys.Rev. C **63**, 024312 (2001).
[76] A. Baran, A. Bulgac, M. M. Forbes, G. Hagen, W. Nazarewicz, N. Schunck, and M. V. Stoitsov, Phys. Rev. C. **78**, 014318 (2008).